NAVAL POSTGRADUATE SCHOOL

MONTEREY, CALIFORNIA

THESIS

DEVELOPMENT AND FEASIBILITY OF EXPENDABLE SPACECRAFT PAYLOADS FOR ACTIVE ORBITAL DEBRIS REMOVAL

by

Connor G. Chroman

December 2023

Thesis Advisor: Giovanni Minelli
Second Reader: Jennifer Hudson

Approved for public release. Distribution is unlimited.

THIS PAGE INTENTIONALLY LEFT BLANK

REPORT DOCUMENTATION PAGE				*Form Approved OMB No. 0704-0188*
Public reporting burden for this collection of information is estimated to average 1 hour per response, including the time for reviewing instruction, searching existing data sources, gathering and maintaining the data needed, and completing and reviewing the collection of information. Send comments regarding this burden estimate or any other aspect of this collection of information, including suggestions for reducing this burden, to Washington headquarters Services, Directorate for Information Operations and Reports, 1215 Jefferson Davis Highway, Suite 1204, Arlington, VA 22202-4302, and to the Office of Management and Budget, Paperwork Reduction Project (0704-0188) Washington, DC, 20503.				
1. AGENCY USE ONLY ***(Leave blank)***	**2. REPORT DATE** December 2023	**3. REPORT TYPE AND DATES COVERED** Master's thesis		
4. TITLE AND SUBTITLE DEVELOPMENT AND FEASIBILITY OF EXPENDABLE SPACECRAFT PAYLOADS FOR ACTIVE ORBITAL DEBRIS REMOVAL				**5. FUNDING NUMBERS**
6. AUTHOR(S) Connor G. Chroman				
7. PERFORMING ORGANIZATION NAME(S) AND ADDRESS(ES) Naval Postgraduate School Monterey, CA 93943-5000				**8. PERFORMING ORGANIZATION REPORT NUMBER**
9. SPONSORING / MONITORING AGENCY NAME(S) AND ADDRESS(ES) N/A				**10. SPONSORING / MONITORING AGENCY REPORT NUMBER**
11. SUPPLEMENTARY NOTES The views expressed in this thesis are those of the author and do not reflect the official policy or position of the Department of Defense or the U.S. Government.				
12a. DISTRIBUTION / AVAILABILITY STATEMENT Approved for public release. Distribution is unlimited.				**12b. DISTRIBUTION CODE** A

13. ABSTRACT (maximum 200 words)

Currently, there are over a thousand large-scale objects in low earth orbit composed of derelict satellites and spent rocket parts that have no means of de-orbiting on their own within a reasonable amount of time and are constantly posing the threat of collision with active spacecraft or other large-scale debris. In the event of collision, these objects have the potential to generate millions of kilograms of dangerous small-scale debris, which is much more difficult to track or to remove. If unchecked, this could lead to a cascade effect of debris generation that would render low earth orbits unusable for active satellites and pose a deadly risk to crewed spaceflight. The focus of this study was to motivate development of an Active Debris Removal spacecraft by reviewing existing technologies, selecting a capture and de-orbit method, and to design and test active debris removal payloads for integration into a commercial-off-the-shelf CubeSat platform. These payloads were then modeled against various real-world derelict objects in order to determine their effectiveness as a potential solution to the orbital debris problem. The harpoon capture method developed in this research was validated as a viable proof of concept, and an electrodynamic tether design was analyzed and determined to be a highly effective method for removing large pieces of orbital debris. This is the first in a series of research projects leading toward an eventual flight mission.

14. SUBJECT TERMS orbital debris, electrodynamic tether, drag enhancement, space harpoon, de-orbit, satellite			**15. NUMBER OF PAGES** 89
			16. PRICE CODE
17. SECURITY CLASSIFICATION OF REPORT Unclassified	**18. SECURITY CLASSIFICATION OF THIS PAGE** Unclassified	**19. SECURITY CLASSIFICATION OF ABSTRACT** Unclassified	**20. LIMITATION OF ABSTRACT** UU

NSN 7540-01-280-5500

Standard Form 298 (Rev. 2-89)
Prescribed by ANSI Std. 239-18

THIS PAGE INTENTIONALLY LEFT BLANK

DEVELOPMENT AND FEASIBILITY OF EXPENDABLE SPACECRAFT PAYLOADS FOR ACTIVE ORBITAL DEBRIS REMOVAL

Connor G. Chroman
Lieutenant, United States Navy
BS, United States Naval Academy, 2016

Submitted in partial fulfillment of the
requirements for the degree of

MASTER OF SCIENCE IN ASTRONAUTICAL ENGINEERING

from the

NAVAL POSTGRADUATE SCHOOL
December 2023

Approved by: Giovanni Minelli
Advisor

Jennifer Hudson
Second Reader

Brian S. Bingham
Chair, Department of Mechanical and Aerospace Engineering

THIS PAGE INTENTIONALLY LEFT BLANK

ABSTRACT

Currently, there are over a thousand large-scale objects in low earth orbit composed of derelict satellites and spent rocket parts that have no means of de-orbiting on their own within a reasonable amount of time and are constantly posing the threat of collision with active spacecraft or other large-scale debris. In the event of collision, these objects have the potential to generate millions of kilograms of dangerous small-scale debris, which is much more difficult to track or to remove. If unchecked, this could lead to a cascade effect of debris generation that would render low earth orbits unusable for active satellites and pose a deadly risk to crewed spaceflight. The focus of this study was to motivate development of an Active Debris Removal spacecraft by reviewing existing technologies, selecting a capture and de-orbit method, and to design and test active debris removal payloads for integration into a commercial-off-the-shelf CubeSat platform. These payloads were then modeled against various real-world derelict objects in order to determine their effectiveness as a potential solution to the orbital debris problem. The harpoon capture method developed in this research was validated as a viable proof of concept, and an electrodynamic tether design was analyzed and determined to be a highly effective method for removing large pieces of orbital debris. This is the first in a series of research projects leading toward an eventual flight mission.

THIS PAGE INTENTIONALLY LEFT BLANK

TABLE OF CONTENTS

LIST OF FIGURES

THIS PAGE INTENTIONALLY LEFT BLANK

LIST OF TABLES

THIS PAGE INTENTIONALLY LEFT BLANK

LIST OF ACRONYMS AND ABBREVIATIONS

18 SDS	18th Space Defense Squadron
ADR	Active Debris Removal
CFSCC	Combined Force Space Component Command
EDT	Electrodynamic Tether
ESA	The European Space Agency
GEO	Geostationary Orbit
LEO	Low Earth Orbit
NASA	The National Aeronautics and Space Administration
NPS	Naval Postgraduate School
NORAD	North American Aerospace Defense Command
ODPO	Orbital Debris Program Office
RPO	Rendezvous and Proximity Operations
SDA	Space Domain Awareness
SSA	Space Situational Awareness
SSN	United States Space Surveillance Network
STK	Systems Tool Kit
USSPACECOM	United States Space Command
USSTRATCOM	United States Strategic Command

THIS PAGE INTENTIONALLY LEFT BLANK

ACKNOWLEDGMENTS

I would like to express my sincere thanks to my advisor, Dr. Gio Minelli, for his invaluable guidance, expertise, and especially for his patience. His support has been crucial to my work. I am also deeply grateful to my wife, Renee, for her constant love, support, and encouragement. Her role in my life has been vital, and reaching this milestone would not have been possible without her and the love of my two boys.

THIS PAGE INTENTIONALLY LEFT BLANK

I. INTRODUCTION

This research builds on previous and ongoing work from the scientific community regarding active debris removal within Low Earth Orbit (LEO). This study reviews several capture mechanisms to capture derelict objects that have been proposed and developed, to include the implementation of a harpoon concept similar to one pioneered by the European Space Agency (ESA) and the Surrey Space Centre [1], [2]. Additionally, there has been significant research into the concept of a scalable drag-enhanced de-orbit device which increases the drag area presented by a spacecraft to aid in its de-orbit [3]–[5]. After examining various existing methods for capturing and de-orbiting objects, this project aims to incorporate these techniques into payloads designed to integrate with commercially available CubeSats.

After designing the spacecraft in modeling software, its effectiveness in active debris removal will be simulated against various real-world debris identified as most concerning by several Space Domain Awareness (SDA) organizations [6]. The targets chosen for simulation vary in size and altitude, in order to determine an effective range and target against which the Active Debris Removal (ADR) payload is most successful. Upon completion of the simulations, the effectiveness as a potential low-cost solution to the orbital debris issue will be determined.

By modeling a prototype expendable spacecraft with the ability to conduct active debris removal against real world debris, this project will provide a proof-of-concept in implementing existing debris removal techniques into a single small satellite. If the design proves cost-effective, the project will provide a path for the scientific community to field numerous active debris removal spacecraft to de-orbit dangerous large objects which currently threaten assets in LEO. In doing so, the creation of further small-scale orbital debris can be avoided, reducing the risk of cascading collisions.

A. BACKGROUND ON ORBITAL DEBRIS

Over the past fifty years, activities in the space industry have led to over 4,800 launches, placing approximately 5,000 satellites into orbit [7]. Of this colossal number, over a thousand large scale objects remain in orbit around the earth, to include active and defunct satellites, rocket bodies, and various expended parts. Besides this significant amount of space hardware, equating to roughly 6,000 tons, myriad other objects are also known to orbit the Earth as a result of collisions in orbit. The U.S. Space Surveillance Network (SSN) consistently monitors all of these space objects, cataloging more than 16,000 of them [7]. These objects vary in size from around 5 to 10 centimeters in LEO and 30 centimeters to a meter in Geostationary Orbit (GEO) [7]. Among the cataloged orbital population, a mere 6% comprise operational spacecraft, while 28% consist of decommissioned satellites, exhausted upper stages, and mission-related objects [7]. The remaining 66% is derived from over 200 on-orbit fragmentations documented since 1961, primarily generating an estimated 700,000 objects larger than 1 cm [7]. High impact velocities, reaching up to 15 km/s for the majority of LEO missions, account for the destructive force despite the orbiting objects' diminutive sizes [7]. Today, there is a growing apprehension that collisions could become the predominant source of new debris, potentially initiating a chain reaction that may render specific orbital zones too hazardous for operations.

Studies conducted between 1991 and 2001 suggest that the number of objects in orbit around the Earth will increase exponentially due to collisions among existing space objects. In certain LEO altitudes where the number of objects exceeds a critical spatial density, debris generation from collisions is greater than the rate of object loss due to orbital decay [8]. The current LEO debris population has already reached a level of severe instability, with collisions expected to be the leading mechanism for future debris generation. Even without new launches, collisions are predicted to persist in the LEO environment for the next 200 years, mainly driven by elevated collision activities between 900- and 1000-km altitudes, which result in a rapidly increasing number of debris objects [8]. The situation is anticipated to deteriorate further due to ongoing spacecraft launches, particularly with massive, proliferated LEO constellations like Starlink and Kuiper.

Although the scientific community has acknowledged this problem since the 1990s, the space community's reluctance to undertake debris remediation activities is primarily attributed to four concerns: the costs associated with debris remediation alternatives are uncertain and potentially high while their performance remains unverified; the rights to manipulate and remove objects registered to other states in terms of ownership and access are ambiguous and potentially controversial; a multi-national forum has not clearly identified the objects most in need of remediation to improve space safety and ensure long-term space sustainability; and attempts to remove or reposition a massive derelict object carry the potential for unanticipated debris generation [6].

The more challenging aspect of the orbital debris issue lies in addressing small-scale, untraceable objects that pose a significant threat to operational spacecraft. However, a more feasible solution focuses on the active removal of large objects before they become involved in collisions that could generate an abundance of smaller debris. By targeting these large-scale objects for removal, the potential for further fragmentation and an increased population of hard-to-track debris can be mitigated, thus alleviating the overall severity of the orbital debris problem.

Research by the National Aeronautics and Space Administration (NASA) and the European Space Agency (ESA) posits that environmental stabilization can be achieved by removing around 10 objects per year from LEO, targeting mass in the removal sequence [9]. Active removal can be more efficient in terms of preventing collisions per object removed by adhering to the following criteria when selecting removal targets, as presented in [7]:

- Opt for objects with high mass (as they pose the most significant environmental impact in the event of a collision)
- Choose objects with elevated collision probabilities (e.g., those situated in densely populated regions)
- Give precedence to objects in higher altitudes (where the orbital lifetime of the resulting fragments is extended).

B. KESSLER SYNDROME

From the beginning of the space program through the 1970s, it was understood that the U.S. government monitored all artificial objects in Earth's orbit, with catalogued objects representing the main collision threat to functioning spacecraft [10]. In 1978, Kessler and Cour-Palais published a pivotal paper titled "Collision Frequency of Artificial Satellites: The Creation of a Debris Belt." This paper suggested that if the catalogued population's growth rate continued, by approximately the year 2000, a significantly more dangerous environment of small debris would promulgate due to fragments from random collisions among catalogued objects [10]. These new debris fields would swiftly create operational risks exceeding those from natural meteoroids, and over time, small debris growth would become exponential, even if no new launches were to take place [10]. Soon after the paper's release, North American Aerospace Defense Command's (NORAD) John Gabbard introduced the term "Kessler Syndrome" to define the future collisional cascading events detailed in the study [10].

The concept of collisional cascading of orbiting objects did not stem from orbital debris research; instead, it originated from studies on the solar system's formation, planetary ring development, and meteoroids and meteorites' emergence from asteroids [10]. Fundamental orbital mechanics principles establish that any two objects orbiting at the same distance from their central body constitute an unstable condition, which occurs because the objects will eventually collide, shattering into numerous smaller fragments and subsequently raising the total number of objects sharing the same distance, thus increasing the collision rate at an exponential rate [10]. The quantity and size of these fragments depend on the collision velocity, which in turn primarily relies on the objects' orbital inclinations; a higher inclination leads to increased collision velocities, producing a greater number of smaller objects that more frequently collide with larger objects [10].

During the early phases of the collision process, the majority of the mass and total surface area is concentrated within larger objects, meaning collisions among these larger entities is the dominant force in converting them into a cloud of smaller fragments [10]. Over time, the sheer volume of smaller objects produced prompts a shift in the distribution of total surface area, which becomes increasingly dominated by these smaller particles and leads to their collisions becoming the prevailing factor in the process [10]. Additionally, each collision reduces both the eccentricity and inclination of the overall debris field until an orbiting dust disk eventually forms around the equator of the central body, similar to Saturn's rings [10].

Three decades ago, there was limited data concerning the repercussions of collisions between large scale artificial orbital objects [10]. The available information predominantly originated from investigations focused on enhancing spacecraft resilience against meteoroids or examining the fragmentation patterns of extraterrestrial rocks. Over the last thirty years, ground-based experiments have been carried out to determine the debris size distribution generated from orbital collisions and to pinpoint the threshold for catastrophic debris-generating collisions [10]. Tests conducted by the military of several countries including the United States, China, Russia, and India involving deliberate orbital collisions have also provided additional insights to this area of study [9].

In order to categorize collisions based on the volume of debris generated, the outcomes of collisions among catalogued objects can be classified into three distinct types:

1. **Negligible Non-catastrophic**: These collisions exhibit minimal impact on both the long-term and short-term orbital environment. They produce an inconsequential amount of debris, which has been previously disregarded in modeling efforts [10].

2. **Non-catastrophic**: These collisions primarily influence the short-term environment. Typically, a non-catastrophic collision occurs between a fragment and an intact object, generating debris approximately 100 times the mass of the impacting fragment [10]. A substantial portion of the mass is transformed into sizes too small for cataloging yet still poses a risk to operational spacecraft. Only a handful of the fragments may be large enough to catalog, thus not significantly contributing to long-term collisional cascading, but potentially posing a considerable short-term hazard to operational spacecraft [10].

3. **Catastrophic:** This type of collision affects both the short-term and long-term orbital environment. A catastrophic collision generates a small-scale debris population similar to that of a non-catastrophic collision, as well as a collection of larger-scale debris that substantially contributes to collisional cascading [10].

In the event of a collision between two objects at or close to orbital velocities, the outcome is expected to be catastrophic [10]. However, when a fragment collides with an intact object, the extent of damage resulting from the collision is determined by the mass of the fragment, a factor that poses a considerable degree of uncertainty [10].

Unquestionably, the repercussions of the so-called "Kessler Syndrome" serve as a significant factor contributing to future space debris, as anticipated over three decades ago. Despite the development of innovative operational approaches during this period, which have mitigated the accumulation of orbital debris, these techniques have been inadequate in halting the growth of the debris population arising from collisions [10]. In order to effectively counteract this escalation, it is crucial to achieve near-perfect compliance with the regulatory guidelines instituted more than a decade ago, and, furthermore, to remove a number of large-scale objects currently in orbit [10]. Luckily, by concentrating on the removal of the most likely sources of future debris, the rate of recovery may be feasible, provided that at least 90% of upcoming launches adhere to existing debris mitigation protocols — a standard that has yet to be fulfilled [10]. Adherence to current guidelines and the deployment of an active debris removal program is the only way in which future spacecraft operators will avoid an irreversible orbital debris problem [10].

This thesis is structured into five chapters, each focusing on a specific aspect of the research. The second chapter provides an in-depth examination of the current technological landscape. It emphasizes the importance of clearly defining the problem and provides a review of the existing methods employed for capturing and de-orbiting space debris. Chapter III details the designs selected and developed for capturing large debris objects using the CubeSat form factor, as well as the selected de-orbit mechanism. The fourth chapter presents an account of various testing procedures and simulations that have been conducted, to include the prototyping phase and the testing of the capture mechanism, as well as a detailed analysis of the de-orbit mechanism when applied to real-world debris objects. The final chapter delves into the practical feasibility of the designed system. It critically evaluates the effectiveness of the proposed solutions and also identifies potential avenues for future research in this topic.

II. CURRENT TECHNOLOGY

A. SPACE DOMAIN AWARENESS

Space Domain Awareness (SDA) is a critical component in the management of orbital debris. The term denotes the ability to identify, track, and predict the movement of objects in orbit around the Earth. This includes operational satellites, defunct satellites, spent rocket bodies, and other fragments, collectively known as space debris. With an estimated count of over 128 million debris objects larger than 1mm, the importance of SDA in preserving the safety and long-term sustainability of the space environment is abundantly clear [1].

Space Domain Awareness necessitates the involvement of various global agencies, each playing a significant role in tracking, monitoring, and mitigating the risk associated with orbital debris. These agencies, with their specialized knowledge and resources, are integral to our collective understanding and handling of the space debris problem. They spearhead research, develop technologies, and implement policies to not only track and catalog space debris but also strategize for its active removal. This section will delve into the roles and responsibilities of several key SDA agencies, providing an overview of their contributions to orbital debris management and the broader implications for space traffic management. A clear understanding of these entities and their policies is crucial, as it shapes our current capabilities and strategies for active orbital debris removal and sets the groundwork for the future actions necessary to ensure the long-term stability of space operations.

1. United States Space Command

As the appointed custodian of SDA and Space Situational Awareness (SSA) for the United States government, the United States Space Command dedicates itself to fostering a space environment that epitomizes safety, security, sustainability, and stability [11]. This commitment is realized primarily through the extensive dissemination of SDA information. The SSA Sharing Program, originally launched by the United States Strategic Command (USSTRATCOM) in 2009, encapsulates this commitment [11].

The program provides an all-encompassing range of cost-free SSA data and services, covering every aspect from pre-launch preparation to end-of-life disposal of a satellite. In 2019, the stewardship of this program transitioned to USSPACECOM. The SSA Sharing Program shares basic SSA data publicly via the website www.space-track.org, which can be accessed by all.

USSPACECOM delegated the management of this initiative to the Combined Force Space Component Command (CFSCC). While CFSCC maintains oversight of the program, the day-to-day responsibility of SSA data sharing and support has been allocated to the 18th Space Defense Squadron (18 SDS) [11]. The 18 SDS also functions as the principal liaison between satellite operators and the U.S. Department of Defense [11].

2. NASA's Orbital Debris Program Office

NASA's Orbital Debris Program Office (ODPO), located at the Johnson Space Center in Houston, Texas, was established in 1979 and has since been recognized as the leading non-military U.S. governmental authority on artificial space debris [12]. This office's primary mission involves providing leadership in national and international initiatives aimed at mitigating the increasing threat posed by orbital debris. One of its major responsibilities is conducting extensive research and development programs aimed at comprehending the environmental implications of orbital debris and potential impacts. This involves studying the current environment, creating models to predict future debris scenarios, measuring debris properties, and researching effective mitigation strategies.

A crucial role that the ODPO plays is in measuring the orbital debris environment. This is achieved using ground-based and space-based assets, which include radar and optical telescopes [12]. The ODPO also uses in-situ measurements and examines spacecraft surfaces returned from space to gather data on smaller debris fragments that cannot be tracked but can still pose significant risks to spacecraft. The ODPO is also deeply involved in predictive modeling of orbital debris. For instance, it develops models such as the LEGEND (LEO-to-GEO Environment Debris) model, which is instrumental in simulating the future debris environment [12]. Parameters considered in these models include variables such as launch traffic, explosion events, collision events, and the potential effectiveness of mitigation measures [12].

Mitigation strategies are another crucial aspect of the ODPO's mission. The office devises and advocates policies and guidelines to minimize the generation of new debris. These standards, which address areas such as mission planning, mission operations, and post-mission disposal of spacecraft and rocket bodies, have been adopted by many space agencies and organizations across the globe [12]. The ODPO is also responsible for developing techniques and materials to protect spacecraft from debris strikes.

In addition to these tasks, the ODPO also takes on an international leadership role, representing NASA and the U.S. government in global forums related to orbital debris [12]. This role involves collaborative work with other national and international space agencies, along with commercial entities, to share information and formulate global solutions to the orbital debris problem.

3. European Space Agency Space Debris Office

The European Space Agency's (ESA) Space Debris Office spearheads research efforts across key domains of space debris such as measurements, modeling, protection, and mitigation. It collaborates extensively with national agencies including the Italian Space Agency (ASI), the British National Space Centre (BNSC), the French National Centre for Space Studies (CNES), and the German Aerospace Center (DLR). Together, they constitute the European Network of Competences on Space Debris (SD NoC) [13].

The European Space Agency (ESA) has two main centers focused on space debris: the European Space Operations Centre (ESOC) in Germany and the European Space Research & Technology Centre (ESTEC) in the Netherlands [13]. At ESOC, the team is skilled in tracking debris, running simulations, assessing risks, and managing a database on space debris [13]. They also work on ways to reduce debris and analyze the risks of space collisions and falling debris. Meanwhile, the team at ESTEC is focused on detecting debris impacts in space, studying the effects of these impacts, and developing technologies to protect spacecraft from high-speed debris collisions [13].

The Space Debris Office of ESA played a leading role in the inception of a European Space Surveillance System. This project has now evolved into an introductory program for a more comprehensive SSA program [13]. The office supports the SSA program's research activities, focusing on aspects like sensor design, performance requirements, and catalog maintenance. Providing operational support for both future and current missions within ESA and for third parties is a major responsibility of ESA's Space Debris Office. This encompasses a range of services like avoiding collisions while in orbit, forecasting re-entries and evaluating associated risks, and managing the Database and Information System Characterizing Objects in Space (DISCOS), which monitors all detectable objects [13]. Additionally, the Space Debris Office has developed a suite of engineering tools dedicated to space debris analysis. These user-friendly software solutions include MASTER-2005, which forecasts the flux of debris and meteoroid particles along specified orbital paths, PROOF-2005 for orchestrating and simulating campaigns to observe debris using radar and optical methods, and DRAMA, which assists in ensuring that space missions adhere to established debris mitigation standards [13].

Beginning in 1984, the European Space Agency (ESA) has played a pivotal role in either hosting or supporting various global conferences focused on space debris. These events encompass the European Conferences on Space Debris, which are held every four years, as well as gatherings organized by the Committee on Space Research (COSPAR), the International Astronautical Congress (IAC), and the International Association for the Advancement of Space Safety (IAASS) [13].

4. LeoLabs Incorporated

Founded in 2016 and headquartered in Menlo Park, California, LeoLabs, Inc. is a private company providing services to mitigate the risks associated with satellite operations in LEO [14]. LeoLabs has created a platform that offers high-quality mapping and analytical services to support SDA and Space Traffic Management (STM) initiatives.

LeoLabs operates a global network of phased-array radar systems that continuously track objects and debris in LEO. These systems use state-of-the-art technology to provide high-resolution data and predictive modeling of the orbital debris environment [14].

LeoLabs' primary service is to provide access to this data, which is vital for satellite operators, regulatory bodies, and space agencies that need to track satellites and space debris.

In addition to the current and forecasted locations of all tracked objects in LEO, LeoLabs also offers collision avoidance services. These services provide early warnings to satellite operators about potential collisions with other satellites or space debris. The company can issue alerts up to a week before potential collisions, allowing operators time to decide if they need to maneuver their satellites to avoid a collision [14]. To ensure global coverage, LeoLabs operates radar facilities at strategic locations around the world. These sites enable LeoLabs to continuously scan the skies, providing an up-to-date picture of LEO space at all times [14].

LeoLabs is unique in that it provides SDA on a scale to match those of national agencies, but as a private commercial business. This marks the beginning of what could be a lucrative private venture, lowering the economic burden on a government, similar to how SpaceX has transformed the government-commercial interface for launch and data services. LeoLabs' contributions are critical in an era where the number of satellites and other objects in LEO is rapidly increasing due to the rise of mega constellations, space exploration missions, and commercial space activities.

5. Global Space Domain Awareness Policies

On the international level, the United Nations Committee on the Peaceful Uses of Outer Space (COPUOS) and its subcommittees deal with matters related to space debris, space traffic management, and the long-term sustainability of outer space activities [15]. COPUOS serves as a global forum where international space policies and legal instruments are formulated, and its primary purpose is to promote the peaceful uses of outer space [15]. COPUOS consists of 95 member states, reflecting its widespread and growing significance in the global landscape [15]. In recent years, the role of COPUOS has evolved to address the challenges brought about by the increasing commercialization of space activities, the growing problem of space debris, and the need for improved space traffic management [15]. It remains committed to nurturing global conversations and collaborative efforts to guarantee that the exploration and utilization of outer space are conducted for the collective advantage of all nations and for generations to come.

The Inter-Agency Space Debris Coordination Committee (IADC) is an international governmental organization that aims to address the growing concern of space debris [16]. Established in 1993, the IADC is composed of representatives from 13 space agencies, including NASA (USA), ESA (Europe), Roscosmos (Russia), CNES (France), ISRO (India), CNSA (China), and several others [16].

The main goal of the IADC is to share research findings on space debris among its member space agencies, to create chances for collaboration in this research area, to assess the advancement of current joint projects, and to pinpoint strategies for reducing space debris [16]. The committee convenes once a year and structures its efforts across four main working groups: Measurement, Environment and Database, Protection, and Mitigation [16]. The Measurement Working Group is dedicated to defining the present conditions of space debris, while the Environment and Database Working Group aims at predicting the future debris environment [16]. The Protection Working Group devises strategies to shield spacecraft from space debris, and the Mitigation Working Group explores methods to reduce the generation of new debris [16].

One of the most significant contributions of the IADC is the creation of the Space Debris Mitigation Guidelines [16]. These guidelines detail steps to decrease the chances of in-space breakups, restrict the dispersal of objects related to missions during regular activities, lessen the risk of collisions while in orbit, and guarantee that non-operational spacecraft do not disrupt the utilization of important orbital paths. [16]. These guidelines have been endorsed by the UN COPUOS.

Despite the extensive national and international efforts, there is currently no comprehensive, globally accepted SDA and STM policy framework. Various international stakeholders, including government, commercial, scientific, and civil society entities, are persistently striving towards achieving this objective, recognizing its critical importance for the future of space activities.

B. ORBITAL MECHANICS

The challenge of orbital debris removal extends beyond mere engineering complexities, delving into deep scientific considerations anchored in orbital mechanics. To begin, this section elucidates the intricacies of Earth's upper atmosphere by exploring its components and dynamics, highlighting its variability with factors like altitude and solar activity. Here, the emphasis is on understanding how drag influences orbital lifespan and how its effects can be precisely computed using our detailed atmospheric models. Finally, the section concludes with a brief discussion on rendezvous and proximity operations, which is integral to the problem but outside the scope of this research.

1. Atmospheric Modeling

Predicting the atmosphere in space is a complex endeavor due to the rarified nature of this environment and the multitude of factors that influence it. Despite the numerous models developed to approximate the atmosphere, they often possess an inherent uncertainty, with error margins hovering around 10–15% [17]. Generally, these atmospheric models are founded on three primary methodologies. The first method leverages empirical measurements, assessing the decay of satellites in orbit over time [17]. The second method utilizes data sourced from ground-based observations, particularly focusing on the flow of charged particles and their interactions with the Earth's magnetic field. The third approach stems from general circulation models that apply fluid flow principles to describe the upper atmosphere's dynamics [17]. Notably, these methods are predominantly empirical, typically relying on databases or look-up tables informed by prior data or existing models. The scientific community remains divided on the superiority or validity of one model over another, illuminated in Figure 1 [17]. However, achieving a reasonably accurate representation of the upper atmosphere is paramount, especially as most of the common de-orbiting mechanisms rely on drag-induced de-orbiting.

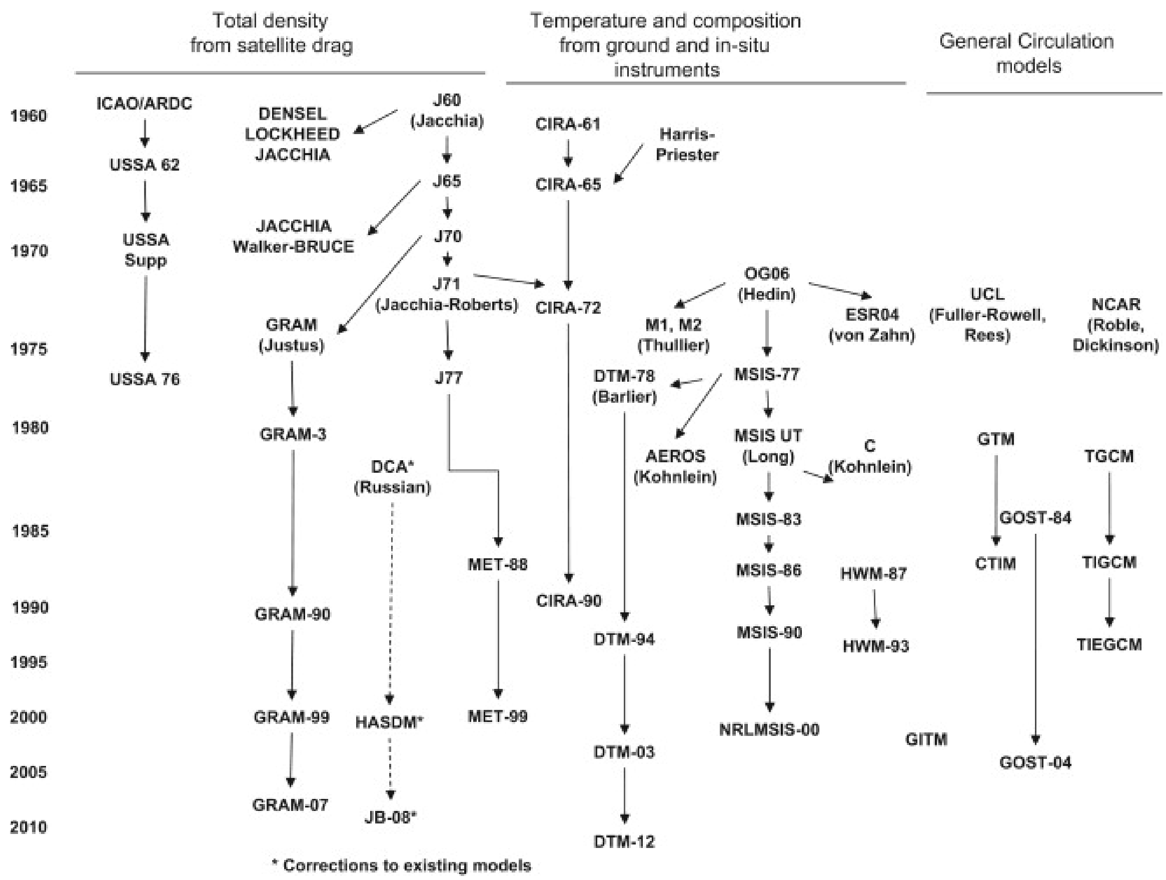

Figure 1. Development of Atmospheric Models. Source: [17]

The upper atmosphere spans several layers, including the troposphere, thermosphere, and extends into the exosphere. Our primary interest lies between 65–1000 km above the Earth's surface. Beneath the 65 km threshold, reentry forces become so intense that they will destroy spacecraft unless they are specifically designed to withstand them [17]. Conversely, beyond 1000 km, the atmosphere's density is minimal, exerting negligible impact on spacecraft operations over meaningful durations [17]. For the strategy of drag-induced de-orbiting to be both effective and dependable, operations typically are employed from altitudes ranging between 800 km to approximately 250 km. Once within this lower boundary, a spacecraft is poised for reentry within weeks or even days, contingent on various factors [17]. As such, it is necessary to select an atmospheric model that provides the highest accuracy for our simulations at these altitudes and below.

In this study, the focus will be on atmospheric models available within the Systems Tool Kit (STK) Lifetime Tool by Ansys Government Initiatives (AGI). Among the available options, three models stand out as particularly noteworthy for consideration: Jacchia 1970, Naval Research Laboratory Mass Spectrometer Incoherent Scatter Radar 2000 (NRLMSISE-00), and Drag Temperature Model 2020 (DTM 2020) [18]. The selection of an appropriate model should consider both the recency of the data it uses and its reliability. A more recent model is often preferable, as it draws upon a larger and more updated dataset, enhancing its predictive accuracy [18].

For these reasons, the Jacchia 1970 model, being static and outdated, can be excluded from consideration [18]. In contrast, The NRLMSISE-00 model represents a significant advancement over its Jacchia predecessors in several key aspects. One of the most noteworthy enhancements is the incorporation of a broader range of data sets into the NRLMSIS database [19]. Unlike the Jacchia models, which were primarily based on drag measurements, the NRLMSISE-00 model includes ground-, rocket-, and satellite-based measurements. These measurements include the use of incoherent scatter radar (ISR), mass spectrometers, and solar ultraviolet (UV) occultation techniques. Additionally, the database incorporates real orbital decay information, which served as the foundation for the Jacchia models, along with new collections of data on temperature and molecular oxygen number density. These new collections are comprehensive in terms of volume, spatial extent, and the duration they encompass, marking a substantial evolution from the MSIS database that was employed to develop earlier versions of the model. [19].

Moreover, the NRLMSISE-00 model responds to the intensity of geomagnetic activity and offers a prediction of the average state of the upper atmosphere during conditions of geomagnetic storms [19]. This makes it more versatile and accurate in capturing the complexities of the Earth's upper atmosphere.

The DTM 2020 model represents a significant leap in the field of atmospheric modeling, particularly in its ability to provide more accurate density estimates. One of the key features that sets DTM 2020 apart from its predecessors, such as NRLMSISE-00, is its incorporation of data from accelerometer-equipped satellites like GRACE and Swarm A, as well as a variety of other data sets, including those from GOCE, CHAMP, and Stella, among others [20]. These data sets include orbital information from satellites in orbit between the year 2000 to 2019, providing a comprehensive view of atmospheric conditions over nearly two decades.

As a result, DTM 2020 densities are on average 20–30% smaller than those of previous models and shows a smaller standard deviation in the yearly mean density ratios when compared to other models [20]. The model also employs different combinations of solar and geomagnetic indices, making it more adaptable and precise. Its densities are more aligned with real-world observations, making it a superior choice for studies requiring high levels of precision, such as calculating orbital lifetime [20]. Therefore, for the specific requirements and objectives of this study, the DTM 2020 model will serve as the basis for calculating orbital lifetime.

2. Rendezvous and Proximity Operations

Rendezvous and Proximity Operations (RPO) play a crucial role in missions aimed at removing orbital debris. While the topic is expansive enough to merit its own comprehensive study—especially when it comes to dealing with large debris—this research will only touch upon it briefly. The section that follows offers a concise overview of RPO's significance in the context of active orbital debris removal.

a. Rendezvous

The concept of rendezvous in space operations is a multi-faceted process that involves aligning the orbit of one object, known as the "chase object," with that of another object, termed the "target object" [21]. The ultimate aim is to bring the chase object to the target object, a condition known as "phasing." The rendezvous process is categorized into three distinct but interrelated phases: Orbit Alignment, Orbit Shaping, and Orbit Phasing [21].

The first phase, known as "Orbit Alignment," serves as the foundation for the entire rendezvous process. During this phase, the primary objective is to align the orbital planes of the chase object and the target object. This involves matching the right ascension of the ascending nodes (RAANs) and the inclinations of both orbits [21]. Achieving this alignment is crucial because any misalignment would require additional maneuvers later in the process, consuming more fuel and complicating the mission [21]. The Orbit Alignment phase sets the stage for the subsequent phases by ensuring that both objects are in the same orbital plane, thus making it easier to approach and interact with each other [21].

The second phase is “Orbit Shaping,” where the focus shifts to matching the shapes of the orbits of the chase object and the target object [21]. The shape of an orbit is characterized by parameters such as the semi-major axis, eccentricity, and argument of perigee [21]. During this phase, the chase object performs a series of maneuvers to adjust these parameters so that its orbit closely resembles that of the target object [21]. This is a critical step because a mismatch in orbit shapes would make it challenging to maintain a stable relative position between the two objects, thereby complicating any subsequent operations.

The final phase is “Orbit Phasing,” which involves positioning the chase object at a specific point in its orbit relative to the target object [21]. The relative phase angle between the two objects is measured in terms of their true anomalies. The chase object performs maneuvers to adjust this relative phase angle until it meets the specific requirements for rendezvous [21]. Once this relative phase angle is achieved, the orbits are considered “phased,” and the chase object can proceed to execute proximity operations with the target object [21].

Interestingly, these phases need not be executed in a strict sequence [21]. They can be mixed and matched to achieve efficiencies, particularly in terms of fuel consumption. For instance, it is possible to combine shaping and phasing in the same set of maneuvers to save fuel [21]. The concept of rendezvous is critical in various space missions, debris removal being most critical to this study. A thorough understanding of these phases and their interplay is essential for the successful execution of any mission involving rendezvous. As such, the rendezvous process is not just a set of maneuvers but a complex orchestration that requires a deep understanding of orbital mechanics, precise calculations, and strategic planning.

b. Proximity Operations

Proximity operations are activities conducted in close quarters with another space object after rendezvous. These operations are categorized into various patterns, each with its own set of challenges and requirements [21]. These patterns are essential for mission planning and execution, as the choice of pattern significantly impacts the mission's objectives, complexity, and resource requirements.

The first pattern, "Linear Drift," involves the chase object maintaining a constant relative velocity to the target object, effectively drifting along a straight line when observed from the target object 's frame of reference [21]. This is a straightforward approach that is often used for simple inspection or observation missions where intricate maneuvers are not required. The second pattern, "Natural Motion Circumnavigation," is more complex and leverages gravitational forces and orbital mechanics to maintain a path around the target object without the need for active propulsion [21]. This pattern is particularly useful in missions where fuel efficiency is a critical concern, as it minimizes the need for active maneuvers [21]. The third pattern, "Drifting Natural Motion Circumnavigation," combines elements of both drifting and natural motion. In this pattern, the chase object not only circumnavigates the target object but also drifts relative to it [21]. This creates a more complex path that is often used in missions requiring detailed inspections of multiple aspects of the target object.

The fourth pattern, "Forced Motion Circumnavigation," involves the chase object being actively propelled to move around the target object [21]. Unlike Natural Motion Circumnavigation, this pattern requires active control and propulsion systems to maintain the circumnavigation path, making it suitable for missions where precise control is needed. The fifth pattern, "Way-Point Flying," involves the chase object moving between specific points relative to the target object [21]. This pattern is often used for inspection missions where the chase object needs to examine multiple points around the target object. The chase object moves from one waypoint to another, stopping or slowing down as needed to perform its tasks. The final pattern, "Station Keeping," is one of the most challenging patterns as it requires the chase object to maintain a fixed position relative to the target object [21]. This is particularly difficult due to the natural forces, like gravity and atmospheric drag, that act upon the chase object and could move it away from its intended position.

Target objects can be categorized into three distinct types based on their level of cooperation with the chase object: “cooperative,” “non-cooperative,” and “uncooperative” [21]. A “cooperative” target object is one that actively assists the chase object in its mission. This assistance can be passive, such as markings or beacons that make it easier for the chase object to identify and approach the target object, or active, such as emitting radio signals to guide the chase object’s navigation systems or active maneuvering to assist the chase object [21]. On the other hand, a “non-cooperative” target object neither assists nor hinders the chase object [21]. It is essentially a neutral entity in the operation, requiring the chase object to rely solely on its own resources and capabilities to complete the mission. Lastly, an “uncooperative” target object is one that takes active measures to prevent the chase object from successfully conducting proximity operations [21]. This could include evasive maneuvers or even countermeasures that disrupt the chase object’s systems.

A prime example of a “non-cooperative” target object in the context of space operations would be orbital debris. They are essentially inert objects floating in space, following their orbital paths due to gravitational forces. When a mission aims to remove such debris, the chase object has to perform all the tasks—ranging from identification and approach to capture or deflection—without any assistance from the debris itself. This makes the mission inherently challenging, as the chase object must have sophisticated sensing, tracking, and maneuvering capabilities to successfully complete the operation.

Since the primary objective of this study is to explore cost-effective strategies for removing orbital debris, one of the key considerations in achieving cost-effectiveness is to minimize or entirely eliminate the use of propulsion systems on the chase object, as these systems can significantly drive-up operational costs. To this end, specific patterns of proximity operations—namely Linear Drift, Natural Motion Circumnavigation, and Drifting Natural Motion Circumnavigation—are likely to be the focus of the design approach. These patterns are particularly advantageous because they require minimal propulsion, thereby aligning with the cost-saving goals [21].

Moreover, these patterns could potentially be executed through a technique known as “differential form flying” or “differential drag” [22]. In this approach, the chase object adjusts its orientation to either increase or decrease aerodynamic drag, effectively inducing motion relative to the target, which in this case is the debris object [22]. By skillfully manipulating the chase object’s orientation, it may be possible to achieve the desired proximity operation patterns without the need for active propulsion systems [22]. This technique could be useful while the latch mechanism on the chase object attempts to capture the debris, potentially allowing for precise, yet low-cost, maneuvering. While developing detailed calculations and precise maneuvers required for rendezvous and proximity operations on orbital debris, propulsion-free or otherwise, lays outside the scope of this study, it does identify this as a promising avenue for future research.

C. CAPTURE MECHANISMS

Debris capture mechanisms are the linchpin of any successful ADR mission, serving as the interface between the debris and the removal spacecraft. These mechanisms must be robust, adaptable, and precise, capable of securely capturing targets of varying sizes, shapes, and conditions under the unique constraints of the space environment. The complexity is further compounded by the uncooperative nature of the debris, which may be tumbling or spinning, lacking standardized docking interfaces, and situated in orbits fraught with collision risks.

This section aims to provide an overview of the state-of-the-art debris capture mechanisms, categorizing them based on their operational principles—whether they require a pushing or pulling maneuver for de-orbit. Technologies such as tethered systems employing throw-nets and harpoons, pushing systems utilizing clamping mechanisms and propulsion, as well as contact-less methods like ion-beam shepherding, will be examined in detail [7]. Each mechanism’s advantages, limitations, and suitability for specific mission profiles will be critically assessed.

1. Pulling Technologies

Among the various technologies being explored for ADR, pulling mechanisms such as nets and harpoons stand out for their potential effectiveness and adaptability. Net capture systems utilize specially designed nets to ensnare uncooperative space debris, often incorporating propulsion systems and winches to secure and control the captured object [7]. These nets can be designed to wrap around and entangle the target, ensuring a secure capture. On the other hand, harpoon systems employ a projectile mechanism to puncture and capture the debris. These harpoons are typically tethered to the capturing spacecraft and can be reeled in after successful engagement [7]. Both net capture and harpoon systems offer unique advantages and challenges, from the precision required in targeting to the mechanisms for ensuring a secure capture and subsequent de-orbiting.

a. Net Capture Systems

In essence, a net capture system employs a net that is ejected from a spacecraft, in this case the chase object, towards the target debris. The net is designed to open up in space and envelop the object, with deployment masses at the corners of the net ensuring that it wraps around and securely entangles the target [7]. In some designs, the net is equipped with motor-driven winches that reel in the neck of the net to prevent it from reopening, thereby ensuring a secure capture [7]. Once captured, the net and the ensnared debris can be tensioned by the spacecraft and de-orbited in a controlled manner, often accelerated by a drag-inducing de-orbit mechanism detailed in the next section.

In 2013 ESA conducted a comprehensive analysis on the viability of de-orbiting space debris through a tethered net mechanism [23]. Utilizing multibody simulations with several thousand degrees of freedom, the study scrutinized the entire de-orbit process, encompassing both the capture and pulling phases [23]. It affirmed that the use of an elastic tether makes de-orbit plausible in both single- and multi-burn scenarios. The elasticity of the tether was found to simplify controller design and enhance control authority, particularly at the end of the burn phase [23]. The proposed net, fabricated from a high strength-to-weight ratio material like Dyneema, measured 16 by 16 meters with a mesh size of approximately 20 centimeters. The net would be deployed from a canister and expanded by corner masses, and would envelop the target debris just prior to impact, driven by the inertia of the corner masses. While simulations indicated that passive net closure would likely suffice, the study also suggested the possibility of implementing a simple closing mechanism for added security [23]. Overall, the study identified no significant barriers to the implementation of the tethered net mechanism for capturing and de-orbiting space debris, thereby underscoring its promise and feasibility [23].

b. Harpoon Capture Systems

The concept of utilizing a harpoon mechanism for debris capture is a compelling concept lauded for its simplicity, compactness, and lightweight design [24]. In essence, a projectile is fired from the spacecraft towards the target debris to capture it. Many current models involve either compressed gas or controlled pyrotechnics to fire the projectile, which has a tether secured to it [24]. One of the key features of the harpoon is its ability to be relatively target agnostic. The projectile could be fired at debris in any orientation and still remain latched if properly penetrated, and the projectile could be barbed to ensure that once the debris is captured, it remains firmly in place, mitigating the risk of escape [24]. Once the harpoon successfully attaches to the target, the attached tether could be tensioned, facilitating the controlled de-orbiting or relocation of the captured debris.

The feasibility of a harpoon system has been substantiated through rigorous on-ground testing involving real structural elements of satellites and rocket bodies [25]. These trials have demonstrated the concept's practicality and effectiveness. Moreover, the system's design is inherently flexible, with various design variants under consideration to simplify its integration into ADR missions, mostly concerning projectile types but also involving the firing mechanism [25]. This flexibility is particularly important given the wide range of debris types, which necessitates a versatile solution capable of capturing multiple kinds of objects without requiring design modifications.

In testing, both on ground and in orbit, the harpoon system emerges as a promising, versatile, and practical solution for the capture of space debris, thereby positioning it as a strong candidate for future ADR missions.

2. Pushing Technologies

In an effort to examine different facets of debris mitigation, pushing technologies offer an interesting alternative to traditional pulling mechanisms. This section introduces these innovative approaches, specifically highlighting the clamping method and contactless technologies such as Ion-Beam Shepherding. The clamping method employs specialized mechanisms to securely embrace the target debris before making physical contact, while contactless methods leverage forces exerted from a distance to manipulate debris [7]. Both approaches aim to address the unique challenges associated with capturing and de-orbiting non-cooperative orbiting objects, thereby expanding the toolkit for effective space debris removal.

a. Clamping Method

In contrast to strategies that involve pulling orbital debris, another approach focuses on pushing the target into a de-orbit trajectory. This method is particularly innovative in its use of a "capture before touching" technique, inspired by three decades of research in docking mechanisms [7]. The core of this strategy lies in a specialized clamping mechanism on the spacecraft, designed to encircle and secure the debris before any physical contact is made. This feature not only mitigates risks related to collision and attitude control but also eliminates the need for the debris to have specific docking structures, which most of the target debris would not have [7].

The ultimate goal is to form a rigid composite between the spacecraft and the debris in preparation for the de-orbiting phase. Once latched, the spacecraft would activate its propulsion system, either a liquid or solid fuel thruster, to guide the debris out of orbit [7]. However, this approach is not without its challenges. It requires a more complex and robust rendezvous maneuver compared to pulling methods previously discussed. Precise sensors would be required to measure the relative positions and velocities between the spacecraft and the debris, and the operation would likely be conducted without direct ground control, adding another layer of complexity [7].

Preliminary evaluations, including multi-body simulations, have been conducted to assess the feasibility and effectiveness of this clamping method [7]. While the approach shows promise, it is significantly more complex and requires further study to address its inherent challenges.

b. Ion-Beam Shepherd Method

Emerging as a departure from traditional methods of docking or capturing space debris, "contactless technologies" have gained attention as an innovative and experimental approach. While the term "contactless" may be somewhat misleading, these technologies present a viable alternative for debris removal, although they come with certain limitations in momentum transfer capabilities [7]. Among these, the Ion-Beam Shepherd (IBS) method stands out for its potential.

Originally developed for spacecraft acceleration, IBS uses ion thrusters to propel charged particles at high speeds, adapting this technology to transfer momentum to non-cooperative space debris [7]. During a mission, the spacecraft would approach the target debris and maintain a consistent along-track distance. It would then direct one ion beam at the debris to create a continuous drag force, while simultaneously aiming another ion beam in the opposite direction to preserve the relative distance between the two objects [7]. This allows for the maneuvering of space debris without the need for physical contact.

Preliminary studies indicate that the IBS method is fundamentally viable and offers several advantages, such as the capability of a lightweight IBS spacecraft to de-orbit large debris weighing several tons, and minimal efficiency losses when a 10–15m along-track distance is maintained [7]. However, the approach also includes many challenges, including the difficulty of maintaining a stable co-orbit with non-cooperative debris and the beam force's dual effects of stabilization and destabilization [7]. Further research is essential to comprehensively evaluate the IBS method's feasibility and effectiveness in practical scenarios.

D. DE-ORBIT MECHANISMS

Following successful capture of the object, the next phase of active debris removal involves the de-orbit mechanism, which is responsible for safely guiding the debris from its current orbit to a re-entry or disposal orbit. This section aims to provide an overview of de-orbit mechanisms, categorizing them into two primary types: propulsion-based de-orbiting and propulsion-less de-orbiting. Understanding the nuances, advantages, and limitations of these methods is crucial for the development of effective and efficient debris removal systems.

1. Propulsion-Based De-Orbiting

Propulsion-based de-orbit methods employ the spacecraft's onboard propulsion system to modify the orbit of the target debris. In this approach, the spacecraft expels a specific type of propellant, generating thrust in the opposite direction to induce a change in the debris' velocity and, consequently, its orbit. The nature of the propellant can vary and may include options such as chemical propellants, ionized gases, or electrically charged particles, each with its own set of advantages and disadvantages.

One of the primary considerations for this method is the need for an adequate supply of propellant to be stored onboard the spacecraft. The quantity of propellant required is contingent upon multiple factors, including the mass of the debris, the desired change in orbital parameters, and the efficiency of the propulsion system [23]. Storing a sufficient amount of propellant necessitates careful planning and design, as it directly impacts the overall weight of the spacecraft. This, in turn, has implications for the launch costs, as heavier payloads are more expensive to send into orbit.

Additionally, the complexity of the system increases with the incorporation of a propulsion-based de-orbit mechanism. The spacecraft must be equipped with the necessary hardware to store, manage, and expel the propellant. This includes fuel tanks, pressure regulators, and thruster assemblies, among other components [23]. The integration of these elements demands meticulous engineering to ensure reliability and safety, especially given the high-risk nature of active debris removal missions.

Propulsion-based de-orbiting techniques can be employed in conjunction with various capture mechanisms to secure the target debris, the most closely associated of which being clamping methods [23]. Once a firm attachment is established, the spacecraft can then activate its thrusters to initiate the de-orbit process. Both solid and liquid fuel thrusters are viable options for this purpose, each offering distinct advantages. Solid fuel thrusters are generally simpler and more reliable but offer less control over thrust levels [7]. Liquid fuel thrusters, on the other hand, provide greater control over thrust magnitudes and durations but are more complex and require additional subsystems for fuel storage and management [23].

A critical aspect of using propulsion-based de-orbiting with clamping methods is the need for precise knowledge and alignment of the system's center of gravity. This is crucial because the thrusters must generate a force that passes through the combined center of gravity of the spacecraft-debris system to avoid rotational perturbations [23]. Even a minor offset in the center of gravity can lead to unintended torques, causing the debris to spin or tumble uncontrollably [23]. Such perturbations could not only jeopardize the de-orbit mission but also pose additional risks of collision or fragmentation, exacerbating the orbital debris problem.

Tether-based capture mechanisms, including nets and harpoons, are also able to utilize propulsion-based de-orbit strategies. In these scenarios, the spacecraft's thrusters are used to generate a pulling force rather than a pushing force. One advantage of this approach is that it is less sensitive to the precise alignment of the system's center of gravity compared to clamping methods [7]. Because the tether allows for some flexibility in the relative positions of the spacecraft and the debris, minor offsets in the center of gravity are less likely to result in destabilizing torques or rotations [7].

However, the use of tethers introduces its own set of challenges. One primary concern is the potential for tangling, especially if the debris is rotating or has irregular geometry. A tangled tether could compromise the mission and may even result in the creation of additional debris. Moreover, the tether itself can introduce rotational forces into the system. If not properly managed, these rotational forces could lead to complex dynamical behaviors, such as oscillations or spins, that could make the de-orbit maneuver more challenging to control and execute successfully [7].

2. Propulsion-Less De-Orbiting

In contrast to the complexities and resource requirements associated with active, propulsion-based de-orbit methods, passive de-orbit techniques offer a simpler and more cost-efficient alternative. These methods capitalize on the natural drag forces present in LEO to facilitate the de-orbit process by utilizing drag-inducing devices that, once deployed, increase the drag force experienced by the spacecraft or debris, thereby accelerating its natural orbital decay.

Unlike active methods, passive de-orbit techniques require no ongoing guidance or control systems to execute the de-orbit maneuver. This eliminates the need for complex software algorithms, fuel storage, and propulsion hardware, thereby reducing both the mission's complexity and cost [3]. This section will introduce two primary designs for passive de-orbit methods: the drag sail design and the electromagnetic drag tether design.

The drag sail design is a passive de-orbit method that involves deploying a large, lightweight sail to increase the surface area exposed to atmospheric drag. The underlying principle is straightforward: by increasing the drag force acting on the object, the design accelerates its natural orbital decay [26]. Variants of this design often incorporate extendable or inflatable booms to provide structural support for the sail.

For optimal effectiveness, the sail is oriented perpendicular to the direction of orbital motion. This orientation maximizes the interaction between the sail and the sparse atmospheric particles in LEO, thereby maximizing the drag force [26]. However, maintaining this orientation requires careful planning and, in some cases, active control mechanisms. As such, the drag sail design may not be the most suitable option for systems that are rigidly connected or for debris objects that are tumbling uncontrollably. The inability to maintain the optimal orientation could significantly reduce the effectiveness of the drag sail in hastening orbital decay [26].

Another consideration is the vulnerability of the sail material to perforation. Given the high-speed environment in orbit, even microscopic debris particles can cause damage to the sail. Any perforation or tearing would compromise the sail's structural integrity and could reduce its drag-inducing capabilities, thereby affecting the efficiency of the de-orbit process.

The electromagnetic tether design offers another passive approach to de-orbiting, but it operates on different principles compared to the drag sail design. In this method, a conductive tether is deployed from the spacecraft. Unlike the drag sail, which requires a rigid boom for support, the electromagnetic tether trails behind the spacecraft without the need for any additional structural elements [27].

This design achieves increased drag in two distinct ways. First, the physical length of the tether itself contributes to aerodynamic drag, similar to the drag sail [27]. However, the unique feature of the electromagnetic tether is its interaction with Earth's magnetic field. As the spacecraft orbits within the magnetosphere, the conductive tether cuts through the magnetic field lines, inducing an electromotive force [27]. This leads to the generation of a passive electrodynamic drag force, which acts in addition to the aerodynamic drag to accelerate the de-orbit process [27].

One of the key advantages of the electromagnetic tether design is its orientation-agnostic nature. Unlike the drag sail, which requires careful orientation to maximize drag, the electromagnetic tether is effective irrespective of its orientation relative to the direction of motion [27]. This makes it a more versatile option, especially for debris objects that are tumbling or for missions where precise orientation control is challenging. Furthermore, the absence of a need for structural supports like booms simplifies the design and potentially reduces the overall system weight and complexity.

III. PAYLOAD DESIGN

A. CAPTURE MECHANISM

The previous chapter provided a comprehensive overview of the various methods available for capturing and managing orbital debris. Among the numerous techniques explored, the harpoon method stands out as a particularly promising approach for active debris removal. This method, inspired by the centuries-old practice of hunting or fishing using a harpoon, has been adapted to the unique challenges and constraints of the space environment. The harpoon method involves using a tethered projectile to pierce and secure debris, allowing for controlled retrieval or repositioning. Its potential advantages include precision, scalability, and the ability to capture a wide range of debris sizes. This section will explore the technical intricacies of the harpoon method and the rationale behind its selection for this research.

1. Design Selection

As previously discussed, most of the harpoon capture methods in development rely on a projectile fired using compressed gas. This propulsion mechanism, while undeniably effective, comes with its own set of challenges. Firstly, the use of compressed gas as a propellant requires the inclusion of additional equipment, such as gas storage tanks, release valves, and pressure regulation systems [24]. The integration of these components inherently increases the system's complexity, posing potential challenges in terms of maintenance and reliability.

Secondly, the inclusion of these additional components contributes to an increase in the overall weight of the debris capture system. In the realm of space missions, weight is a critical factor, as it directly impacts launch costs and the maneuverability of the spacecraft in orbit. Recognizing these challenges, and with an overarching goal of developing a cost-effective design, this research focuses on an alternative approach to design a mechanism that can effectively launch the harpoon projectile without relying on any form of pressurized gas propulsion. This design aims to be streamlined and lightweight, making it particularly suitable for integration into smaller satellite platforms such as

CubeSats. CubeSats, given their compact form factor and cost-effective nature, represent a promising avenue for future space missions, and adapting the harpoon capture method to this platform could significantly advance the field of active orbital debris removal. As such, the design was developed to fit within the constraints of a 3U form factor, measuring 10 cm by 10 cm by 30 cm [18].

To create a design that is both compact and lightweight, inspiration was drawn from the harpoon mechanism commonly employed in spearfishing. The design of a spearfishing harpoon is inherently compact, with a linear configuration that seemed particularly apt for integration into the constrained dimensions of a CubeSat payload.

In the context of spearfishing, the harpoon is propelled using the mechanical potential energy stored in elastic bands. These bands are stretched and loaded, and upon release, they rapidly contract, propelling the harpoon forward with significant force. This mechanism is highly effective in the aquatic environments for which it was designed. However, when considering the application of this mechanism in the LEO environment, several challenges arise. The extreme temperatures in LEO, which can fluctuate dramatically between intense heat and cold, can have profound effects on materials, especially elastomers like those used in spearfishing bands [28]. In such conditions, the elastic bands might lose their elasticity, become brittle, or undergo other material changes [28]. This could result in a reduced capacity to store potential energy or even the failure of the band altogether. Consequently, the mechanism, while effective on Earth, might not perform as expected in the harsh conditions of space. As such, another method for storing and releasing potential energy would need to be explored.

In a similar line of thinking, inspiration was also drawn from crossbows. Crossbows function by storing potential energy through the bending and loading of a flexible limb, typically made of wood or fiberglass. When the crossbow is fired, this limb rapidly returns to its original form, releasing the stored energy and propelling the bolt or arrow forward with significant force.

However, upon closer examination, several challenges became evident when considering the application of a crossbow-like mechanism in the space environment.

Firstly, the materials traditionally used in crossbows, such as wood and fiberglass, are also susceptible to the extreme temperature fluctuations in LEO [29]. Just as with the elastic bands in spearfishing harpoons, these materials might undergo changes in their properties when exposed to the intense cold and heat of space. They could become brittle, lose flexibility, or experience other structural changes, potentially compromising their ability to store and release energy effectively. Furthermore, the design of a traditional crossbow does not align with the requirements for a compact and linear configuration suitable for CubeSat integration. Crossbows, by their nature, have a broader and more spread-out design, which could pose challenges in terms of space optimization and integration into a constrained satellite payload. Given these considerations, while the crossbow presented an intriguing concept in terms of energy storage and release, it was ultimately deemed unsuitable for the specific needs of this project.

Ultimately, a combination of a crossbow and a spearfishing harpoon was decided on for the design. This hybrid approach sought to harness the strengths of both mechanisms while mitigating their respective limitations.

To address the challenge of fitting within the compact dimensions of a CubeSat payload, a significant modification was made to the traditional crossbow design. Instead of the broad limbs that characterize conventional crossbows, the design incorporated sets of pulleys. These were configured to allow for an extended travel of the projectile string, ensuring that the mechanism could generate sufficient force to propel the harpoon. This design adaptation ensured that the entire mechanism remained within the ten-centimeter width constraint of a 3U CubeSat payload, while providing the travel length necessary.

Moving away from the elasticity-based energy storage methods of traditional crossbows and spearfishing harpoons, the design opted for metal springs as the primary means of storing potential energy. Metal springs offer a robust and reliable mechanism for energy storage, especially when considering the extreme temperature fluctuations in LEO. Unlike wood, fiberglass, or elastomers, metal springs are less susceptible to material degradation in space conditions, ensuring consistent performance.

The operational principle of the mechanism is relatively simple. As the projectile is loaded, it drives the primary set of pulleys. These, in turn, drive a secondary set of pulleys connected to the metal springs. As these secondary pulleys rotate, they stretch the springs, effectively storing potential energy. When the projectile is ready to be fired, a release mechanism is activated. The stored energy in the springs is rapidly released as they return to their original length. This motion drives the pulleys, which tightens the string, culminating in the forceful propulsion of the projectile forward, ready to capture its target. Figure 2 displays the preliminary design of the mechanism.

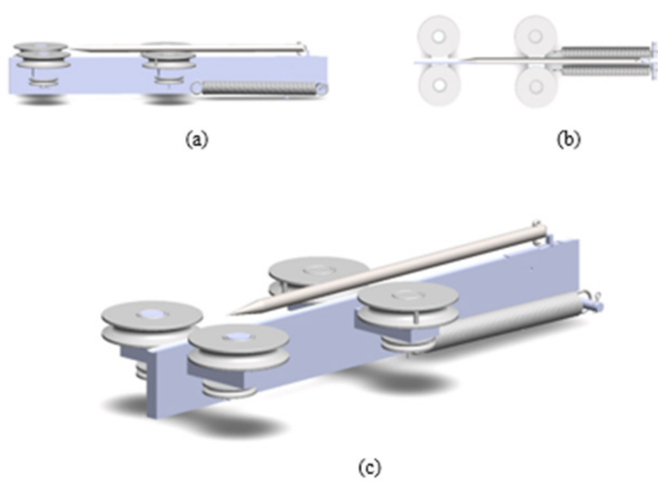

(a) Right Side View, (b) Top View, (c) Isometric view

Figure 2. Preliminary Design

To ensure the harpoon is fired only at the precise moment required, a robust retention and release mechanism was essential. The design criteria for this mechanism were twofold: it must securely hold the release string, preventing premature firing, and it must release the string cleanly and instantaneously when triggered. Moreover, the ability for the mechanism to reset itself automatically after each operation would significantly enhance the system's efficiency and readiness for subsequent use. This would increase the complexity of the design but could have distinct advantages given the high costs and effort needed to put a spacecraft in orbit.

The mechanism that was engineered to meet these requirements is actuated through a lever arm, a simple yet effective solution that allows for a controlled and clean release. This lever arm interacts with a retaining wheel, which is a critical component of the retention system. In its default state, the retaining wheel is held fixed in place, securely locking the release string and preventing any unintended movement. When the lever arm is activated, it triggers a mechanism that allows the retaining wheel to spin freely, thereby releasing the string and propelling the projectile.

The design employs small springs that are integral to the automatic resetting feature of the mechanism. Upon activation, they facilitate the return of the release components to their original positions, readying the system for another cycle without the need for manual intervention. Figure 3 displays the design in both its activated and default state. This design ensures that, barring any material failure, the mechanism can hold the string indefinitely, maintaining the system in a state of readiness.

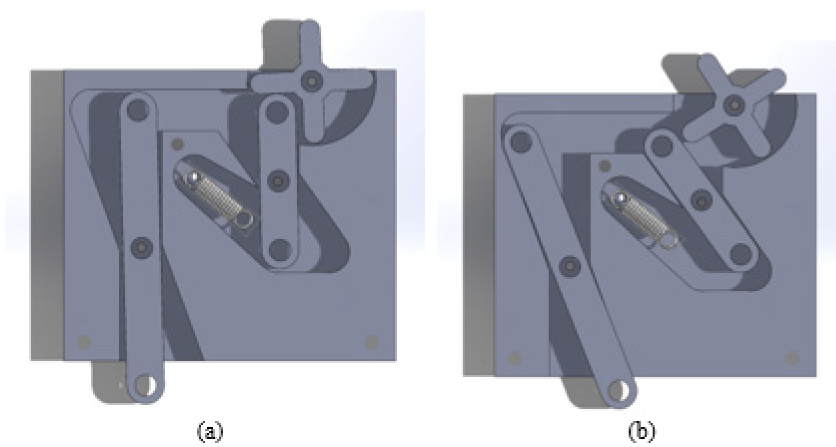

(a) Default State, (b) Activated State

Figure 3. Trigger Release Mechanism

In the space environment, the fact that the objects are in a state of constant freefall presents a challenge for mechanisms that rely on weight or tension to function correctly. This is particularly true for a projectile release system, where gravity on Earth would assist in the separation and movement of components. To adapt to the microgravity conditions of orbit, the initial design was modified to ensure that the projectile could be released smoothly and reliably, without the aid of gravity.

The solution was to double the number of springs in the mechanism and design a barrel-like structure for the projectile. By using four springs instead of two, the system gains redundancy and balance, which helps to counteract the lack of gravitational forces. This adjustment means that the force exerted by each spring can be more evenly distributed, promoting a smoother release action. Additionally, with more springs sharing the load, each spring can have a lower spring constant while still achieving the same total energy output required to propel the projectile.

The updated design, as illustrated in Figure 4, incorporates these four springs along with a barrel through which the projectile is launched. Despite the addition of extra springs, the entire assembly remains compact enough to fit within the confines of a 3U CubeSat form factor.

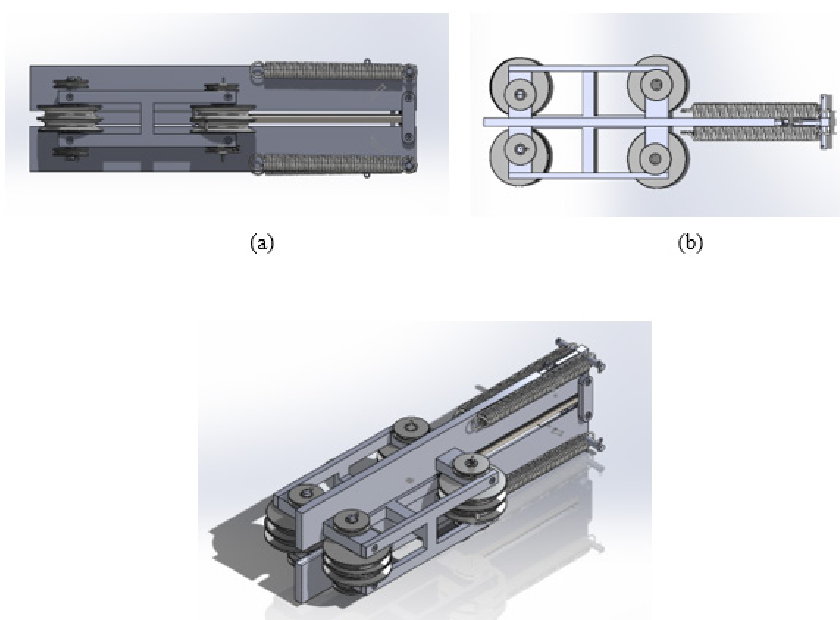

(a) (b) (c)

(a) Right Side View, (b) Top View, (c) Isometric view

Figure 4. Updated Design

2. Spring Selection

In the use of a design such as this in orbital debris removal, the ability of a projectile to penetrate the material of which the debris is composed is critical. Prior research has established that, to address a broad spectrum of debris, the projectile should be capable of penetrating aluminum up to 3 millimeters thick [25]. This thickness is representative of the material used in many satellites and other objects that constitute space debris.

The kinetic energy required for a projectile to reliably pierce through an aluminum plate of this thickness has been quantified through empirical studies. The research indicates that a range of kinetic energy between 206.8 and 220.3 joules is necessary to achieve penetration [25]. However, to ensure reliability across various conditions and to account for any unforeseen variables, a margin of safety is incorporated into the design specifications.

Therefore, to enhance the robustness of the debris removal system and to ensure its effectiveness against a diverse array of targets, the design criteria were set to achieve a kinetic energy delivery of 230 joules. By designing the mechanism to deliver this level of force, the system is expected to perform reliably under a variety of scenarios, ensuring that the projectile can penetrate the target debris as intended.

The potential energy (PE) stored in a spring system can be calculated using

$$PE = \frac{1}{2} k x^2, \tag{1}$$

where PE is the potential energy in joules, k is the spring constant in newtons per meter (N/m), and x is the displacement of the spring from its equilibrium position in meters [30]. When multiple springs are configured in parallel, their individual spring constants combine to form an equivalent spring constant that is the sum of each spring's constant [30]. For four identical springs in parallel, the effective spring constant (K_{eff}) is four times the spring constant of a single spring (k):

$$K_{eff} = k_1 + k_2 + k_3 + k_4 = 4k. \tag{2}$$

To determine the required spring constant for each spring to collectively store 230 joules of energy at a displacement of 12 cm (0.12 meters) for each spring, which is the displacement space available in the design, the potential energy equation is rearranged to solve for *k*:

$$\begin{aligned}
230J &= \frac{1}{2}\left(K_{eff}\right)(0.12m)^{2} \\
230J &= \frac{1}{2}K_{eff}\left(1.44 \times 10^{-2}\,m^{2}\right) \\
230J &= 7.20 \times 10^{-3}\,m^{2}\left(K_{eff}\right) \\
K_{eff} &= \frac{230J}{7.20 \times 10^{-3}\,m^{2}} \\
K_{eff} &= 3.19 \times 10^{4}\,{}^{N}\!/_{m} \\
k &= \frac{K_{eff}}{4} = \frac{31944.44}{4} = 7.99 \times 10^{3}\,{}^{N}\!/_{m}
\end{aligned} \tag{3}$$

To ensure that the mechanism can store the necessary 230 joules of energy, each of the four springs in parallel must have a spring constant of 7.99×10^3 N/m.

B. DE-ORBIT MECHANISM

The preceding chapter provided an overview of various de-orbiting strategies that can be employed once space debris has been securely captured. Among these, the utilization of electromagnetic tethers stands out as a particularly innovative and passive method for the mitigation of space debris. This method distinguishes itself by employing a two-fold mechanism that leverages both aerodynamic and electrodynamic drag forces to significantly hasten the de-orbiting process [27].

The passive nature of this de-orbiting method is one of its most significant advantages and one of the primary reasons for its selection. Unlike active propulsion systems that require fuel and complex guidance systems to maintain or change orientation, electromagnetic tethers require no such active control. This lack of necessity for active propulsion or orientation control systems not only simplifies the spacecraft's design but also reduces the risk of operational failure. Moreover, it contributes to a reduction in mission costs and increases the reliability of the de-orbiting process.

The selection of the electromagnetic tether method is further justified by its established track record and commercial availability, which are critical factors in the context of space missions where reliability and cost-effectiveness are paramount. Tethers Unlimited, a company specializing in space tether technologies, offers these systems as Commercial Off-The-Shelf (COTS) products. The historical deployment of this type of system on the Naval Postgraduate School (NPS) satellite, NPSAT-1, which was launched in 2019, serves as a testament to the method's practical viability [27]. The successful operation of electromagnetic tethers in this mission provides a concrete example of the technology's effectiveness in a real-world space environment [27]. Such a demonstration of capability in an operational context significantly enhances the Technology Readiness Level (TRL) of the system.

The use of flight-tested equipment like that from Tethers Unlimited brings with it the assurance of proven performance. This assurance can lead to reduced costs associated with testing and development, as the need for extensive validation and risk mitigation measures is lessened [27]. In the context of this project, where cost minimization is one of the objectives, leveraging a system with a high TRL can lead to significant savings. Not only does it reduce the need for investment in research and development, but it also minimizes the potential for costly mission failures due to untested or unreliable equipment [27].

Electromagnetic tethers operate on the principle of electromagnetic induction. A conductive tether, when deployed from a spacecraft and extended into space, interacts with the Earth's magnetic field [27]. As the tether moves through the magnetosphere at orbital velocities, it effectively 'cuts' through the Earth's magnetic field lines. This in turn induces a voltage determined by the equation

$$V = \vec{L} \cdot (\vec{v} \times \vec{B}), \tag{6}$$

where V is the voltage induced, $\vec{L}$ is a unit vector in the direction of the deployed tether, $\vec{v}$ is the spacecraft's velocity vector, and $\vec{B}$ is a vector representing the geomagnetic field [30]. This induced voltage, in turn, generates an electric current, which interacts with the magnetic field to produce a force — known as the Lorentz force — that opposes the motion of the tether and the attached debris [30]. The Lorentz force can be modeled with the equation

$$\vec{F} = \int_{0}^{L} (\vec{I} \times \vec{B})\, \mathrm{d}l, \tag{7}$$

where $\vec{F}$ is the Lorentz force, and $\vec{I}$ is the current crossed with the geomagnetic field and integrated along the length of the tape [27]. This force opposes the direction of motion and contributes to lowering its orbit in conjunction with the aerodynamic drag force.

The aerodynamic drag is a result of the physical presence of the tether in the LEO environment, where there are still enough atmospheric particles to create resistance against objects moving at high speeds [27]. The deployment of the tether will increase the spacecraft's cross-sectional area equal to an amount determined by the equation

$$A_{drag,\,tether} \approx \frac{2}{\pi} wL, \tag{8}$$

where w is the width of the tape, and L is the tape's length [27]. The factor of $\frac{2}{\pi}$ accounts for any twist in the tape during deployment or rotation of the system [27]. This increased area can then be used as an input into an orbital decay program to determine how much of a difference in orbital lifetime the deployment of the tether induces. Together, these forces work in concert to slow down the debris, thereby lowering its orbit until it eventually re-enters the Earth's atmosphere and is incinerated.

In summary, the utilization of electromagnetic tethers for de-orbiting space debris offers a passive, reliable, and cost-effective solution to a growing space challenge that is available commercially. With proven commercial viability and a high TRL demonstrated by successful employment on spacecraft like NPSAT-1, this method efficiently accelerates the removal of debris by leveraging natural forces to induce orbital decay [27]. This technology not only aligns with the immediate objectives of sustainable space operations but also hints at a cost-effective option for future employment on a variety of spacecraft.

IV. TESTING AND SIMULATIONS

A. MODELING AND PROTOTYPING

To progress from the theoretical design introduced in Chapter Three to a tangible prototype, the proposed capture mechanism was modeled using Dassault Systèmes's SOLIDWORKS computer modeling system. This advanced modeling platform enabled the precise rendering of the mechanism's details, ensuring adherence to the size constraints imposed by the CubeSat form factor. Following the initial digital design phase, the model was brought to life using a 3D printer provided by NPS's Space Systems Academics Group, a method chosen for its ability to rapidly and cost efficiently produce structures which are often challenging to create using traditional manufacturing techniques.

However, the initial attempts to 3D print the prototype revealed several critical design challenges, primarily stemming from the limitations inherent to the 3D printing process itself. The primary issue encountered was related to the material strength. Given the small scale required for integration into a CubeSat, the materials used in 3D printing did not possess sufficient strength and durability to withstand the stresses involved in creating even a test model, let alone the operational demands expected of the capture mechanism. This was a significant hurdle, as the material had to be robust enough to endure testing and eventually the harsh conditions of space while adhering to the size and weight constraints.

To address these challenges, the design underwent multiple iterations. Each iteration involved reassessing and modifying the design to enhance the strength and functionality of the printed components. This process was iterative and required a balance between the physical properties of the available printing materials and the mechanical requirements of the capture mechanism. Adjustments were made in various aspects of the design, such as the thickness of the components, the use of reinforcement structures, and the replacement of key components like the axels and pulleys with metal versions that could offer greater strength without significantly compromising the size and weight specifications.

The development of the trigger mechanism for the capture device presented a particularly complex challenge in the prototyping phase. Initially, the design of this trigger mechanism was mechanically sound. It functioned effectively in isolation, demonstrating the theoretical viability of the concept. Figure 5 demonstrates its successful prototyping compared to its computer modeling.

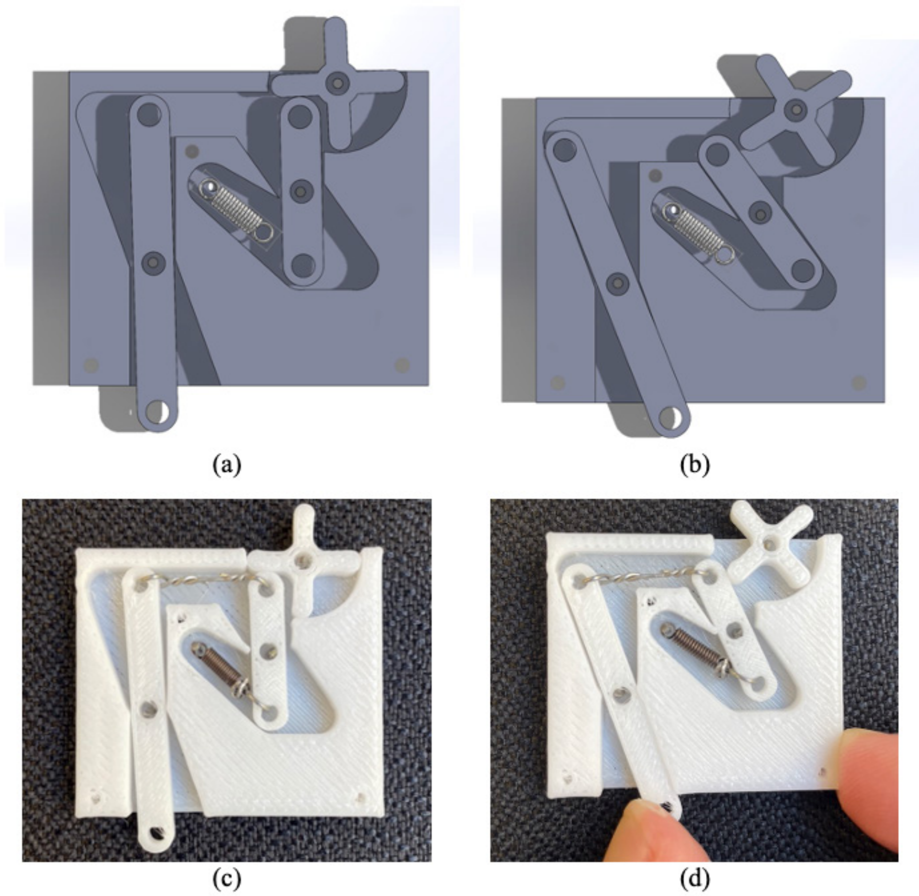

(a) Default state model, (b) Activated state model, (c) Default state prototype, (d) Activated state prototype

Figure 5. Trigger Release Mechanism

However, significant issues emerged when this component was scaled down to the dimensions necessary for integration within the CubeSat form factor and combined with the other elements of the design. At this reduced scale, structural integrity became a critical concern. In the initial prototypes, the material used for the trigger mechanism was found to be too delicate to bear these forces. Over three iterations, the components fractured under stress, rendering the mechanism ineffective. This failure occurred well before the design could be considered ready for testing under simulated operational conditions. As a result, the task of retaining the release cable — a critical function for the success of the capture mechanism — became a significant obstacle.

Given these challenges, the decision was made to designate the refinement of the cable retention aspect of the trigger mechanism as an area for future work. Future efforts in this area would need to focus on identifying and utilizing materials that offer the necessary strength and resilience at the required scale, possibly exploring alternative designs or innovative material compositions that could better meet the operational demands of the trigger mechanism within the stringent size and weight constraints of the CubeSat platform.

In order to create a model to assess proof-of-concept, the decision was made to simplify the test platform for the initial proof of concept phase. This simplification, crucial for isolating and testing the core functionality of the mechanism, involved reducing the design to include only a single set of springs and cables. This approach facilitated a more streamlined examination of the mechanics and operation of the system, allowing for a clearer analysis and troubleshooting process. Additionally, this reduction in complexity significantly eased the fabrication and assembly challenges that had been encountered in earlier prototyping stages. In the final iteration of the prototype design, significant modifications were implemented to specifically address the structural and functional challenges identified earlier, enhancing the strength and durability of the mechanism, particularly in components that were subjected to high stress during operation.

To this end, metal axles were integrated into the prototype, press-fitted firmly into the base structure. This incorporation of metal components was a pivotal improvement over previous versions, which relied solely on 3D printed materials and lacked the necessary strength and rigidity. The support beam for the springs was replaced with metal components. This was a vital modification, as the springs placed considerable stress on their support structure during operation. The metal support beam ensured that the springs were securely anchored and could function effectively without risking structural failure.

A further refinement in the design was the use of metal for the four front sheaves. These sheaves needed to withstand the high tension from the springs and ensure smooth, independent rotation. Replacing these with metal components ensured they could endure the force exerted by the springs while also allowing them to spin freely. Conversely, the four rear sheaves were produced using 3D printing. This decision was based on the need to affix the cord to these sheaves, a requirement that necessitated a level of customization and precision that 3D printing could provide. These rear sheaves were designed to be rigidly connected, allowing them to rotate in unison on each side. As the top cord was pulled to load the projectile, the interconnected movement of the rear sheaves drove the bottom cord system, thereby extending the spring and effectively arming the system. Figure 6 details the model of the test design. With a sturdy prototype now complete, testing could commence.

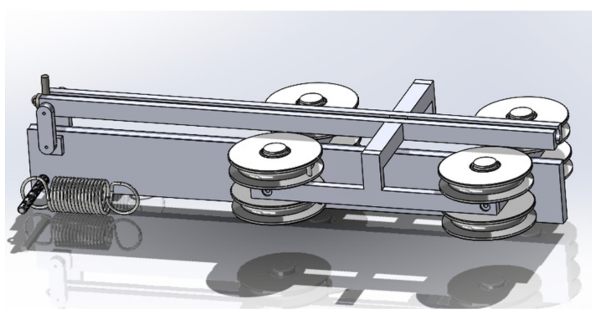

(a)

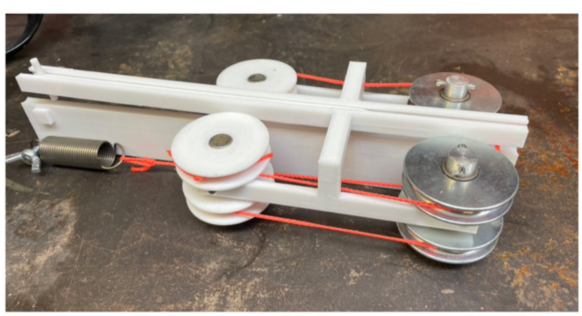

(b)

(a) Test Model, (b) Test Prototype

Figure 6. Capture Mechanism

B. TESTING

1. Methodology

In order to validate the design as a successful proof of concept, testing the efficacy of the scaled-down model was necessary. To do so, the speed of the projectile would need to be measured using the parameters of the test model. This data could then be scaled up using expected operational parameters to determine if the concept would function effectively in orbit.

For testing the capture mechanism prototype, a precise and quantitative method was employed to measure the projectile's speed using high framerate video capture. The setup for the test was carefully arranged to ensure controlled and consistent conditions, detailed in Figure 7. The prototype was securely fastened using a bench vise, stabilizing it to prevent any movement that could affect the accuracy of the measurements. A target was placed at a distance of 65 centimeters from the prototype. This specific distance was chosen to provide a clear path of travel for the projectile and to facilitate accurate measurement of its speed over a known distance.

(a)

(b)

(a) Side view, (b) Top view

Figure 7. Test Setup

A critical part of this test was the measurement of the "muzzle velocity" of the projectile, or the speed at which it leaves the base. To accurately measure this, a distance of 50 centimeters was marked out from the exit point of the base. Additionally, graph paper with a five-millimeter grid was mounted to increase accuracy on either side of the marking during analysis. This marked distance served as a controlled area where the speed of the projectile could be measured effectively.

2. Expected Results

For the purposes of testing, a decision was made to use springs with a lower spring constant than what would be required for actual use in orbit. This adjustment was primarily driven by safety considerations and the desire to preserve the structural integrity of the test model. The high spring rates necessary for orbital operation could pose significant safety risks during ground-based testing and would likely exceed the structural limits of the prototype, which is likely not as robust as the final flight model.

Therefore, two springs, each with a spring constant of 475.59 N/m (2.71 lbs/in), were chosen for the testing purposes. This selection represents a careful balance between achieving a meaningful simulation of the mechanism's operation and ensuring the safety and integrity of the test environment and equipment.

Using the same principles outlined previously, the potential energy stored in this modified system under the test parameters was calculated using the equation

$$
\begin{aligned}
&PE = \frac{1}{2} K_{eff} x^2 \\
&K_{eff} = k_1 + k_2 = 2k = 9.51 \times 10^2 \, {}^{N}\!/_{m} \qquad (9) \\
&\frac{1}{2}\left(9.51 \times 10^2 \, {}^{N}\!/_{m}\right)(0.12m)^2 = 6.85 \, J,
\end{aligned}
$$

where it was determined that the system, with these two springs, would store an expected potential energy of approximately 6.85 Joules.

This level of potential energy, while lower than what would be needed in an orbital scenario, still provides a valuable basis for testing the mechanism's functionality and effectiveness. It allows for the assessment of the prototype's performance under more controlled and less hazardous conditions.

Given that the mass of the projectile is 14.1 grams, the expected velocity of the projectile can be calculated using the kinetic energy equation

$$KE = \frac{1}{2}mv^2$$
$$v = \sqrt{\frac{2KE}{m}} = \sqrt{\frac{2(6.85J)}{1.14\times 10^{-2}kg}} = 34.6\ {}^{m}/_{s}. \tag{10}$$

This approach assumes an ideal system devoid of any energy losses, such as friction or air resistance.

In an ideal scenario, the potential energy stored in the springs is fully converted into the kinetic energy of the projectile at the point of release. By rearranging this equation to solve for velocity and substituting in the values for kinetic energy and mass the expected velocity of the projectile is determined. Under these idealized conditions, without considering energy losses, the projectile's velocity is calculated to be 34.6 meters per second.

3. Actual Results

With the test setup completed and the expected results determined, the projectile was then fired, its movement captured using a high-speed camera recording at 120 frames per second. This high framerate was essential to ensure that each moment of the projectile's flight was captured in detail, allowing for a precise calculation of its speed. By analyzing the video footage frame by frame, it was possible to accurately determine the speed of the projectile as it traveled the specified distance. Figure 8 shows the frames in which the projectile was in motion.

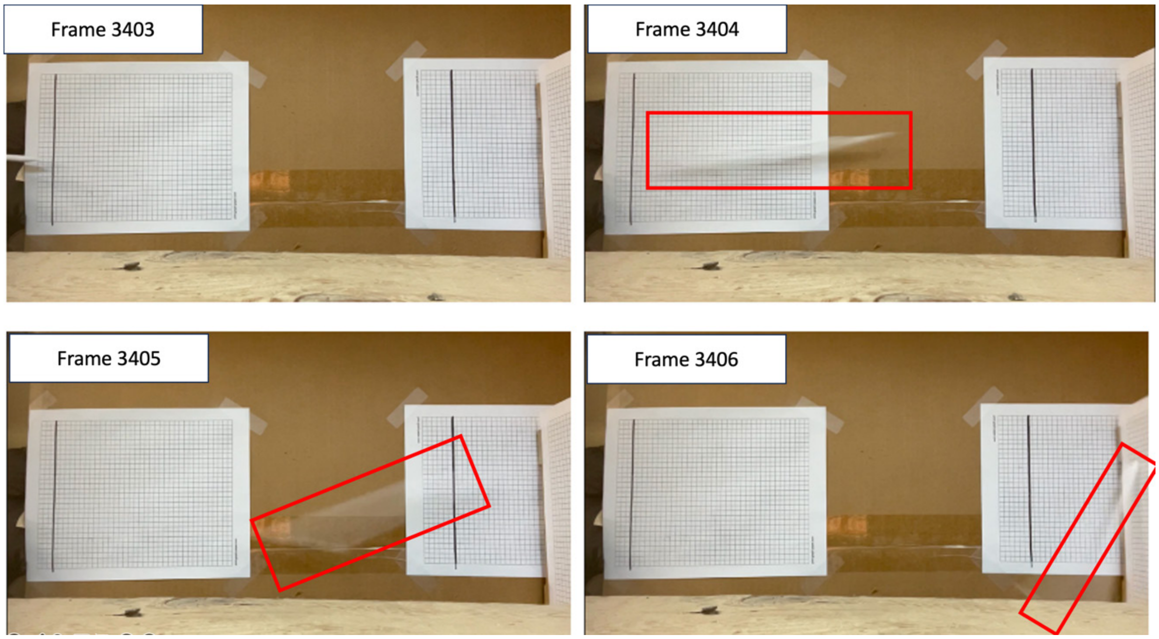

Figure 8. Projectile in Motion.

During the test, the issue of motion blur was encountered in the captured frames. This blur, even though the camera was operating at a high frame rate, introduced a degree of uncertainty into the analysis of the projectile's speed. Frame 3405 in Figure 8 displays the instant that the half meter threshold was crossed. However, due to the motion blur present, there was an inherent uncertainty in pinpointing the exact position of the projectile at this specific moment.

To address this challenge, a more detailed examination of frame 3405 was conducted, using the grid background seen in Figure 9. The grid provided a reference system for measuring the extent of the motion blur more accurately. By carefully analyzing the blurred image of the projectile against the grid lines, it was possible to estimate the position of the projectile with greater precision at the beginning and end of the camera's exposure during the frame. This allowed for a more refined estimation of the projectile's distance traveled, bounding the uncertainty introduced.

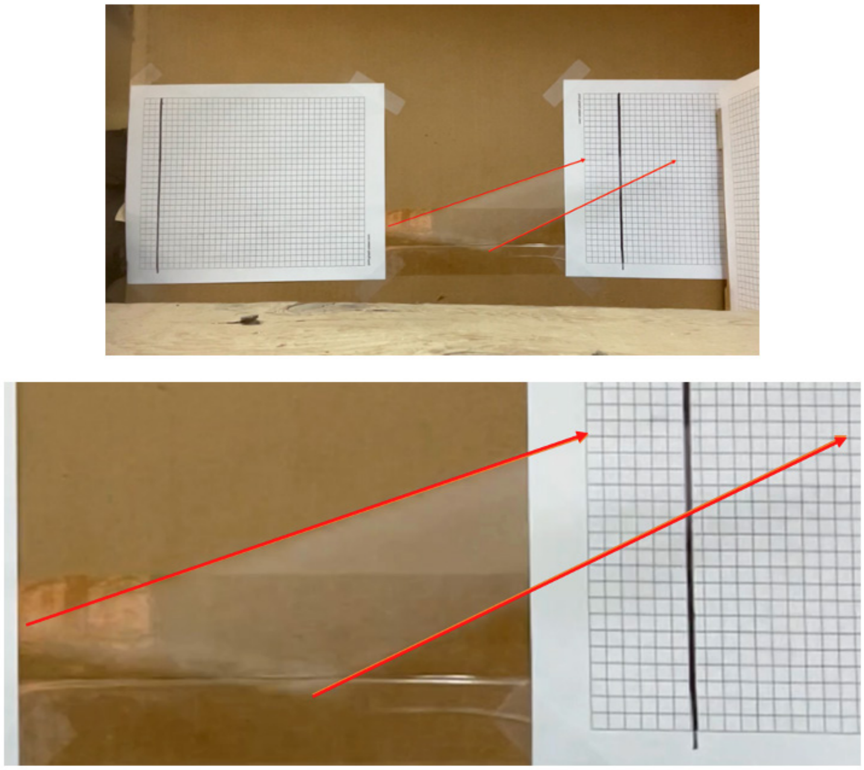

Figure 9. Analysis of Frame 3405

Using the grid, it is clear that for the duration of frame 3405 the projectile was at a distance of either 0.5m – 30 mm or 0.5m + 50 mm, between 0.47 meters and 0.55 meters. Utilizing equation 11, the velocity of the projectile can be determined with known uncertainty:

$$v = \frac{d}{t}$$

$$\frac{0.47\ m}{2\ frames}\left|\frac{120\ frames}{1\ sec}\right. = 28.2\ {}^{m}/_{s} \tag{11}$$

$$\frac{0.55\ m}{2\ frames}\left|\frac{120\ frames}{1\ sec}\right. = 33.0\ {}^{m}/_{s}$$

where v is velocity of the projectile in meters per second, d is distance traveled in meters, and t is the time interval in seconds. Therefore, the velocity of the projectile was determined to be 28.2 to 33 meters per second.

The results from the test showed that the velocity of the projectile closely aligned with the previously calculated ideal velocity of 34.6 meters per second. This close alignment is a significant finding, as it indicates that the prototype performed nearly as expected under the ideal conditions assumed in the theoretical model.

However, there was a slight discrepancy between the theoretical and observed velocities. This discrepancy can primarily be attributed to factors that were not accounted for in the ideal model. These include frictional losses within the mechanism, aerodynamic drag on the projectile, and slight imprecision in the trajectory of the projectile. In a real-world setting, such factors invariably affect the performance of any mechanical system.

Unfortunately, the force generated during the test was so great that it resulted in a cracked frame on the 3D printed prototype. This damage was substantial enough to prevent further testing with this particular model. The occurrence of such structural damage highlights the challenges faced when scaling down high-energy mechanisms to smaller prototypes, especially when using materials like those typically used in 3D printing, which may not have the necessary strength to withstand such forces. It also indicates a need for further refinement in the design, likely involving the use of more durable materials or a reinforced structure to better accommodate the stresses involved in the operation of the mechanism.

Despite these minor deviations, the test results were very encouraging. By achieving a velocity that nearly matched the ideal calculation, the prototype effectively demonstrated the proof of concept. This successful test outcome indicated that the basic principles and designs underpinning the capture mechanism were sound and could be effectively realized in a physical model.

By extrapolating the results from this test model to the operational parameters – specifically, employing four springs with spring constants of 7.99×10^3 N/m – it is projected that the objective of delivering 230 joules of energy could be achieved. This extrapolation is based on the assumption that the flight model will possess adequate structural integrity to handle the higher forces generated by these more robust springs. The success of the prototype thus lays a solid foundation for further development and scaling of the design along the path to a flight mission.

C. DE-ORBIT SIMULATIONS

1. Modeling

The task of modeling the impact of an electrodynamic tether (EDT) on an orbiting object involves complex calculations, primarily due to the unique operational characteristics of the EDT, harnessing both aerodynamic drag and electrodynamic drag derived from the Lorentz force [31]. The complexity of accurately modeling these interactions stems from the dynamic nature of these forces. The aerodynamic drag depends on the atmospheric density at the orbiting altitude, while the electrodynamic drag is influenced by factors like the tether's electrical conductivity, length, orientation, and the velocity of the orbiting body [31]. There have been concerted efforts in the scientific community to develop sophisticated simulators capable of accurately predicting the behavior and performance of EDTs. For instance, the University of Michigan developed the TEthered Mission Planning and Evaluation Software Tool (TeMPEST), and Universidad Carlos III de Madrid created the Bare Electrodynamic Tether Mission Analysis (BETsMA) software [32]. These tools are designed to encapsulate the complex mathematical models that describe the interaction of the tether with Earth's magnetic field and the varying conditions in the upper atmosphere.

However, before the creation of these advanced software programs, analytic methods were used to estimate the performance of EDT systems. One notable contribution in this regard was made by Robert Hoyt, the founder of Tethers Unlimited. Hoyt developed a formula that, while less comprehensive than the models used in TeMPEST or BETsMA, provides an estimation of an EDT's performance. The formula

$$\Delta t = \left(\frac{M_s R}{12 L^2 B_E^2 R_E^6 \cos^2\alpha \left\langle \cos^2\lambda \right\rangle} \right) a^6 \Big|_{a_{initial}}^{a_{final}} \tag{12}$$

offers a more accessible approach to understanding and predicting the behavior of an EDT, albeit with less precision and detail than the more sophisticated simulators [33]. Coupled with the orbital lifetime tool from STK, an estimation of the EDT's performance as a de-orbit device can be analyzed.

To effectively evaluate Equation 12, it is essential to accurately determine several key variables. M_S represents the total mass of the combined debris and spacecraft system, measured in kilograms. L denotes the length of the tether in meters. The performance of the EDT is directly proportional to the length of the tether, with longer tethers generating more force. B_E and R_E are the Earth's magnetic field strength at the equator and radius, measured in tesla and meters respectively. B_E is particularly important for the electrodynamic aspect of the tether, as the interaction of the tether with the Earth's magnetic field generates the Lorentz force. R, the resistance of the tether measured in ohms, is a function of the material's resistivity, in this case, the aluminized multi-layer insulation film tape, its cross-sectional area, and its length. The electrical resistance affects how efficiently the EDT can convert its motion through the Earth's magnetic field into electrical current, which in turn influences the drag force generated. The angle of the tether from the vertical, α, affects the orientation of the tether in relation to the Earth's surface and its magnetic field, which Hoyt and Forward optimally determined as 35.26 degrees [31]. The λ term is a factor of the inclination, and a is the semimajor axis of the debris-spacecraft system measured in kilometers.

Equation 12, once evaluated with these variables, is used to calculate the time required for the debris-spacecraft system to de-orbit from its initial altitude to an altitude of 300 kilometers. This specific altitude is significant because it represents a threshold where the dynamics of de-orbiting change notably [33]. Above this altitude, the effects of electrodynamic drag are the primary factors influencing the de-orbiting process. However, once the system reaches 300 kilometers, aerodynamic forces dominate, taking over from the effects of electrodynamic drag [33]. This marks a transition in the de-orbiting forces acting on the system. The assumptions used in applying Equation 12 are consistent with those in the source paper from which the equation is derived. In this paper, the primary focus is on the effects of electrodynamic drag at higher altitudes. It is assumed that at these higher altitudes, atmospheric drag is so negligible that it does not factor into the timeline analysis of de-orbiting until a lower altitude is reached [33]. It is only when the system descends to an altitude of 300 kilometers or lower that atmospheric drag becomes significantly more effective than electrodynamic drag, replacing electrodynamic force as the primary de-orbiting factor [33]. Additionally, Equation 12 is focused solely on the drag resulting from electrodynamic forces, which is why the ballistic coefficient of the spacecraft is not factored into the analysis until reaching a lower altitude. The ballistic coefficient is only incorporated into the analysis during the STK lifetime simulation after the spacecraft descends to an altitude of 300 kilometers. Until this point, the equation primarily models the performance of the tether system from an electrodynamic perspective, emphasizing how electrodynamic forces influence the spacecraft's de-orbiting process in the higher regions of the Earth's atmosphere.

However, it is important to note that in practical scenarios, atmospheric drag can play a significant role in the de-orbiting of the spacecraft at much higher altitudes than the 300 kilometers used in this estimation. This means that the actual de-orbiting times could be shorter than what is calculated solely on electrodynamic drag effects. This discrepancy highlights the necessity to consider both electrodynamic and atmospheric drag forces for a more accurate and realistic estimation of de-orbiting timelines, especially in the transition zone where both forces are relevant and is the reason exquisite modeling programs exist specifically to model both atmospheric and electrodynamic drag concurrently.

Several simplifying assumptions were made to streamline the computations. Firstly, it was assumed that the orbit of the spacecraft-debris system is perfectly circular. While many of the target orbits under consideration were already nearly circular, likely due to drag forces at perigee circularizing the orbit over time, this assumption significantly simplified the calculation of the reduction in the semi-major axis.

Another assumption pertained to the cross-sectional area of the debris object subject to aerodynamic drag, which was assumed to be ten square meters. This value was chosen to accommodate potential variations in the debris object's orientation and movement such as tumbling, which can affect the effective cross-sectional area exposed to atmospheric drag. By standardizing this area, the analysis could more clearly focus on the impact of other variables, specifically the mass of the debris and its altitude, on the de-orbiting process.

The model was then tested against the same data with the same assumptions provided in the paper to validate its effectiveness, with similar results. A spacecraft at an altitude of 1400 kilometers in an orbit with a 52 degree inclination, using a two-kilometer-long aluminum tether would de-orbit within 40 days, which is consistent with the results from the paper [33].

With the theoretical model established for electrodynamic drag force and its optimistic assumptions set, the next step was to apply this model to actual space missions to assess its real-world applicability. A pertinent example of this application is the case of the NPSAT-1 spacecraft. Launched on June 25th, 2019, NPSAT-1 was inserted into an orbit at an altitude of 720 kilometers and an inclination of 24 degrees, equipped with a de-orbit device developed by Tethers Unlimited: the NanoSatellite Terminator Tape (NSTT) [34].

The NSTT, depicted in Figure 10, is a commercially available de-orbit device designed to effectively facilitate the de-orbiting process of small satellites. It is characterized by its deployed length of 70 meters and a width of 150 millimeters, while maintaining a lightweight profile with a total mass of only 808 grams [35]. Constructed from aluminized multi-layer insulation film tape, the NSTT is engineered for durability and effectiveness in the conditions of space, with electrodynamic properties to generate sufficient electrodynamic and atmospheric drag in the Earth's upper atmosphere, aiding in the efficient de-orbit of attached satellites [35].

Figure 10. NanoSatellite Terminator Tape (NSTT) Housing Unit. Source: [35]

This de-orbit device was deployed eighteen months post-launch, on December 26th, 2020. To determine the effectiveness of the NSTT, two-line element (TLE) data from space-track.org was analyzed. In Figure 11, the altitude of NPSAT-1 over time is plotted, utilizing this TLE data. The graph provides a clear visual representation of the spacecraft's orbital decay. Notably, there is a distinct inflection point observable in the data shortly after the deployment of the NSTT. This point marks the beginning of a dramatic reduction in the spacecraft's altitude, indicating that the deployment of the NSTT had a significant and measurable effect on hastening the de-orbit process.

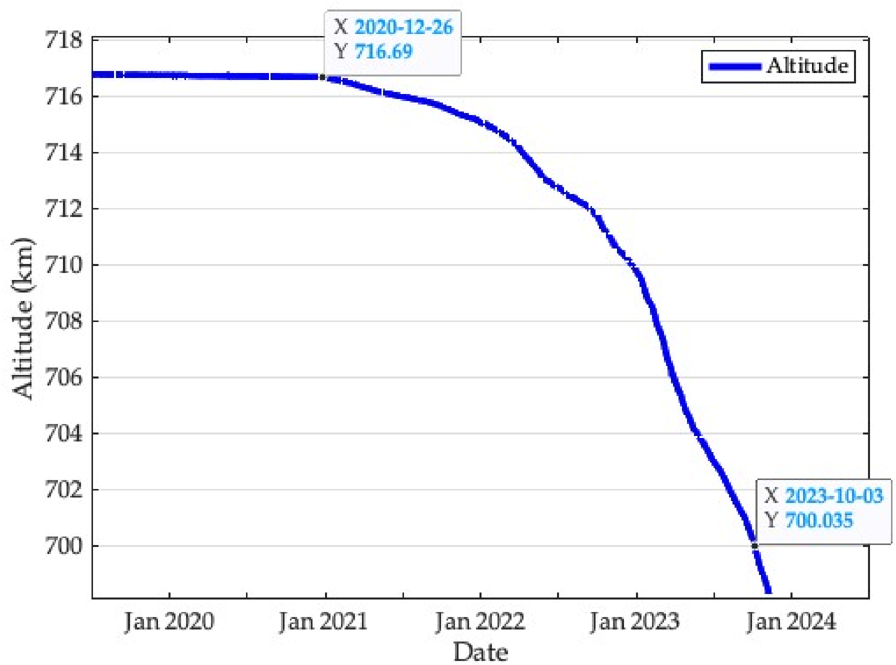

Figure 11. NPSAT-1 Average Altitude over Time

When the NPSAT-1 spacecraft's 82-kilogram mass, 70-meter tether, 720-kilometer altitude, and 24-degree inclination were fed into the theoretical model for electrodynamic drag, it enabled a prediction of the time it would take for the spacecraft to de-orbit to an altitude of 700 kilometers. According to the model, this de-orbiting process was expected to take approximately two years and 13 days from the date of the tether deployment, expecting to cross the 700 km altitude threshold around January 8, 2023, based on electrodynamic drag alone.

However, the actual de-orbiting trajectory of NPSAT-1 differed from this prediction, reaching the 700 km altitude mark on October 3, 2023. This occurred two years, nine months, and eight days after the deployment of the de-orbit device, which is a deviation of eight months and 26 days longer than the model had predicted.

The discrepancy between the theoretical predictions based on a model using only electrodynamic drag and the actual outcomes in space can be explained by various factors. One of the most significant reasons for this difference is the initial model's simplistic exclusion of atmospheric drag or ballistic coefficient. While the model focused solely on electrodynamic drag, it assumed the impact of atmospheric drag to be negligible, particularly at altitudes above 700 kilometers. Surprisingly, the omission of atmospheric drag yielded a theoretical result that was faster than the observed data. While it is true that at these higher altitudes atmospheric drag is considerably weaker compared to the much more dominant electrodynamic drag, even this relatively small amount of atmospheric drag should have contributed to the acceleration of the de-orbit timeline, shortening it by several months compared to predictions based solely on electrodynamic drag [33]. An analysis of the effects of atmospheric drag at high altitudes, such as those proposed when studying differential drag flying, could provide insight into the discrepancy and is an area for future study [36].

In addition, the model was based on ideal conditions, including assumptions of optimal tether angles and perfectly circular orbits. The angle of the tether likely was not the ideal angle used in the model, and no data on the effectiveness of the current flow with the plasma exists for NPSAT-1. Additionally, it did not account for variables such as fluctuations in solar activity, which can significantly impact the space environment and, consequently, the de-orbiting process. Exploring the relationship between solar activity fluctuations and the orbital decay data from NPSAT-1 presents an intriguing area for future research.

Despite these limitations and the observed deviation, the model's prediction was within 30% of the real-world data. This level of accuracy, while not exact, indicates that the model is still a useful tool for estimation purposes. It provides a baseline understanding of the de-orbiting process and a framework for predicting the effectiveness of de-orbit devices like the NSTT. While it is clear that real-world conditions can introduce complexities not fully captured by the model, the overall proximity of its predictions to the actual data suggests its validity as a starting point for estimating de-orbit timelines in similar space missions.

2. Analysis Against Objects of Concern

Having successfully validated the performance estimation model, the research continued to a practical application phase, where the model's effectiveness in real-world scenarios was to be tested. The focus of this phase was to use the model to simulate interactions between a spacecraft equipped with the debris removal system and specific debris objects that are considered high-risk in space. For this purpose, a list created by Darren McKnight, which identified the top 50 most concerning debris objects in orbit, was used as a key reference [6]. This list is significant as it highlights objects that pose considerable risks in terms of their potential for collisions and their overall contribution to the space debris problem.

From this list, five specific debris objects were selected for analysis. The criteria for their selection were based on their distinct characteristics, ensuring that each chosen object was unique in its properties. However, despite their differences, each of these objects represented a broader group of debris on McKnight's list with similar or identical characteristics. This methodical selection meant that, although only five objects were directly analyzed, they collectively represented the characteristics of 43 out of the top 50 objects on the list. The objects chosen were as follows, modeled in Figure 12:

1. **SL-16 Rocket Body** (SATCAT 22566). This spent rocket body was selected because it shares similar characteristics held by the top 20 objects on the list. It has a substantial mass of approximately 9000 kilograms and is in an orbit at around 848 kilometers altitude with an inclination of 71

degrees. Its selection allowed for the analysis of a common type of large, spent rocket body in a relatively high orbit.

2. **SL-16 Rocket Body** (SATCAT 25861). Distinguished by having the lowest altitude in the list, this object's apogee sits at 645 kilometers. It has a higher inclination of 98.2 degrees and possesses a mass similar to the first SL-16 rocket body. The choice of this object offered insights into how lower orbital altitudes affect debris behavior.

3. **COSMOS 2322** (SATCAT 23704). While this object shares a similar orbital path to the first SL-16 rocket body, it has a considerably lower mass of 3250 kilograms. The inclusion of COSMOS 2322 allowed for an examination of how varying masses influence orbital decay, also representing eight other objects on the list with similar characteristics.

4. **ADEOS** (SATCAT 24277). With an inclination of 98.9 degrees, this object had one of the highest inclinations on the list, with mass similar to that of COSMOS 2322 at 3560 kilograms. This selection helped isolate inclination as a variable.

5. **SL-8 Rocket Body** (SATCAT 7594). With a significantly higher apogee of 981 kilometers and one of the lowest masses on the list at 1435 kilograms, this object provided contrast to the others in two regards. Its characteristics are representative of ten of the last objects on the list, allowing for the study of debris in higher orbits with relatively lower masses.

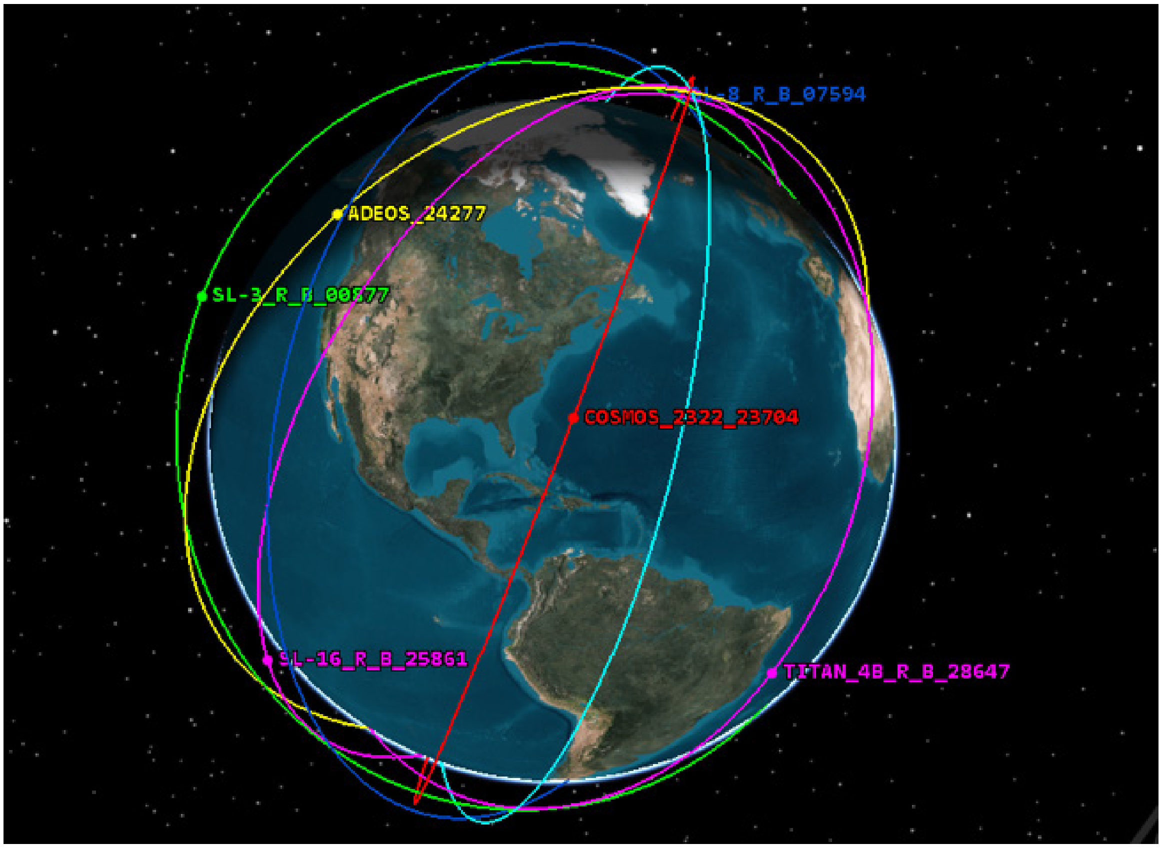

Figure 12. STK Modeling of the Debris Targets.

Each object was modeled in STK without a de-orbit system using the assumptions and parameters previously noted and displayed in Figure 13, and then also modeled with one, three, five, and ten de-orbit spacecraft to assess the effectiveness of a swarm of de-orbit spacecraft acting on these large debris objects. In the scenarios where multiple de-orbit spacecraft are employed, it was assumed that each spacecraft would perform optimally and equally. In real-world conditions, however, such uniform performance is subject to change. Variations in the effectiveness of individual spacecraft could arise due to differences in their operational conditions, capture of the debris object, and placement. These differences could result in some spacecraft contributing more to the de-orbiting effort than others.

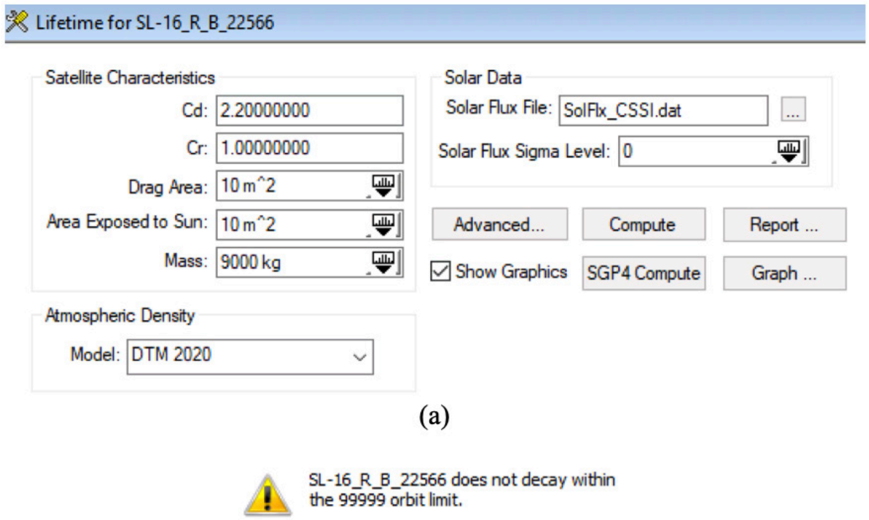

(a) Parameters for analysis. (b) Typical response without de-orbit device

Figure 13. Example Lifetime Analysis Parameters without De-orbit Device for SL-16 Rocket Body 22566

With these assumptions in place, the calculations from Equation 12 were carried out to assess the effectiveness of the EDT system on the pre-selected target orbits. The time to de-orbit from the initial orbit to an altitude of 300 kilometers was modeled using electrodynamic drag alone, and then added to the time to de-orbit from an altitude of 300 kilometers using atmospheric drag alone. The results of these calculations, which provide insights into the potential impact of the EDT on the specified debris objects, are presented in Table 1.

Table 1. De-orbit Times for Selected Targets

SATCAT	Name	Altitude (km)	Inclination (deg.)	Mass (kg)	Deorbit (yrs) Natural	1 S/C	3 S/C	5 S/C	10 S/C
22566	SL-16 R/B	848	71.0	9000	> 250	157.5	53.1	32.2	16.5
25861	SL-16 R/B	645	98.2	9000	> 250	689.6	230.6	139.2	70.4
23704	COSMOS 2322	854	71.0	3250	> 250	57.3	19.4	11.8	6.1
7594	SL-8 R/B	981	82.9	1435	> 250	195.2	66.2	40.5	21.2
24277	ADEOS	794	98.9	3560	> 250	263.6	88.7	53.7	27.4
877	SL-3 R/B	751	65.1	1435	> 250	14.0	4.8	2.9	1.6
28647	Titan 4B R/B	592	57.0	1134	23.2	5.8	2.0	1.2	8.2 months

It was evident from the results that while the spacecraft did contribute to the de-orbiting of the chosen targets, a single spacecraft was not sufficient to make a significant change in the orbits of these objects. Instead, the deployment of multiple spacecraft would be required to achieve a more substantial impact on the de-orbiting process.

A notable finding from the analysis was the influence of orbital inclination on the effectiveness of the EDT. The high inclination of most of the selected debris objects was found to significantly reduce the efficacy of the electrodynamic drag. This reduction in effectiveness is due to the alignment of the debris orbits with Earth's magnetic field lines. Electrodynamic tethers generate force through their interaction with these magnetic field lines, and when an orbit is closely aligned with these lines, the generated force is diminished [31].

To further explore the potential of the de-orbit spacecraft in more favorable orbital conditions, the study extended to include two additional debris objects with lower inclinations, which were not part of McKnight's list. The selected objects were an SL-3 rocket body (SATCAT 877) and a Titan-4 rocket body (SATCAT 28647), with orbital inclinations of 65 and 57 degrees, respectively. These lower inclination orbits are more conducive to the generation of electrodynamic drag, making them better candidates for assessing the full potential of the spacecraft.

The results from analyzing these additional objects were significantly more promising. It was observed that with the deployment of just three de-orbit spacecraft, the debris objects could be de-orbited in under five years. This outcome highlights the importance of selecting appropriate targets for EDT-based de-orbit missions, with lower inclination orbits offering a more effective environment for the technology.

3. Most Effective Use

The analysis of the system's performance in de-orbiting space debris revealed critical insights into the most effective deployment strategy for such de-orbit spacecraft. One of the key findings was the significant impact of orbital inclination on the efficacy of the EDT system. Therefore, the most efficient application of the de-orbit spacecraft would be targeting debris objects in lower inclination orbits, where the full potential of the electrodynamic drag force can be harnessed.

Another important aspect revealed by the analysis concerns the mass of the debris objects. It was found that higher mass objects pose a greater challenge for de-orbit operations. These objects require the deployment of more de-orbit spacecraft to achieve a comparable rate of orbital decay, and consequently, the time needed to de-orbit these larger objects is longer. This is due to the greater momentum and gravitational influence associated with higher mass debris, which necessitates more force for effective de-orbiting.

However, deploying a larger number of spacecraft to expedite the de-orbiting process of heavier debris comes with increased costs. Balancing effectiveness and cost-efficiency is crucial in planning de-orbit missions. The study suggests that using three de-orbit spacecraft strikes a practical balance, offering a reasonable tradeoff between the effectiveness of the de-orbit operation and the higher costs associated with deploying multiple spacecraft. This approach allows for a more efficient and cost-effective de-orbiting of a range of debris objects, making it a viable strategy for mitigating the risks posed by space debris in orbit. Additionally, the use of multiple spacecraft improves the redundancy of the mission in the event of an unsuccessful capture, especially with the implementation of a reset system proposed in the next section that could be considered for future work.

V. CONCLUSIONS

A. FEASIBILITY OF DESIGN

In order to accurately assess the technical feasibility of these payloads and their integration into a CubeSat bus, their Technology Readiness Level (TRL) must be evaluated, depicted in Figure 14.

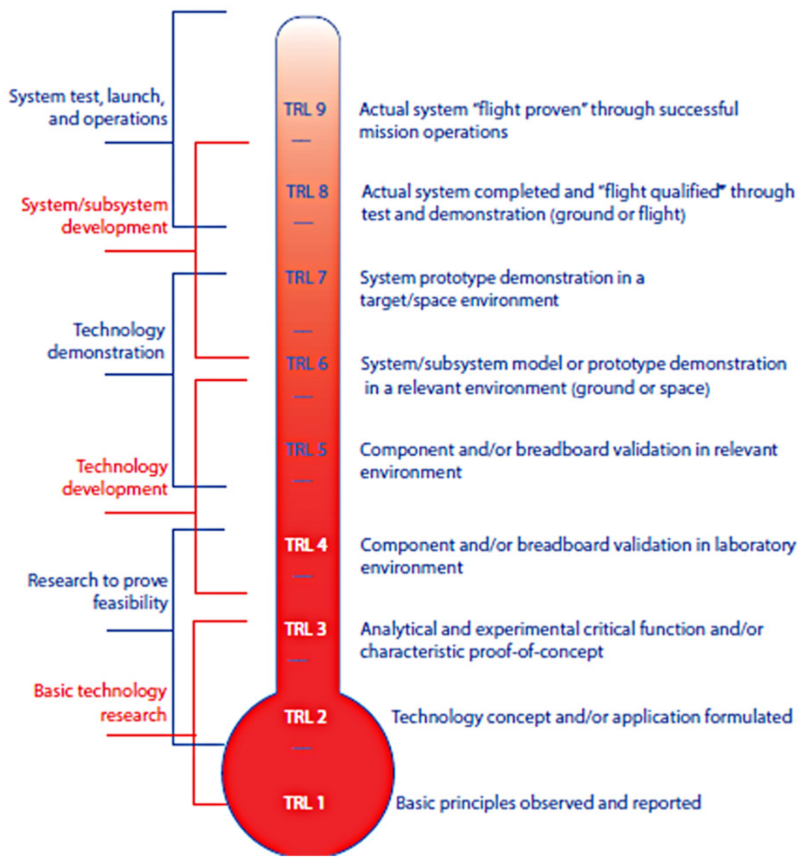

Figure 14. NASA's Standard TRL Scale. Source: [37]

For the EDT proposed in the study, its commercial availability and proven flight heritage are key indicators of its maturity. The fact that it is commercially available implies that the technology has been developed, tested, and is ready for purchase and use. More importantly, its proven flight heritage suggests that it has been successfully implemented and operated in space missions. These factors collectively place the de-orbit component of the design at TRL 9, which is the highest level of technology readiness. This indicates that the EDT is considered fully mature and has been demonstrated to work reliably in a mission environment.

Conversely, the capture mechanism is at an earlier stage of development. The testing conducted can be classified as "analytical and/or experimental critical function proof of concept" [38]. This means that while the concept of the capture mechanism has been proven to work in controlled laboratory conditions, it has not yet been demonstrated in a realistic mission environment. However, without testing in an environment that closely mimics the conditions of space, the technology cannot be considered ready for actual mission deployment. Consequently, the capture mechanism is assessed at TRL 3. This level indicates that the concept is active and has been experimentally validated, but further development and testing are required to advance its maturity for space missions.

In the context of assessing the overall readiness of the system comprising the individual components for a CubeSat mission, it is important to consider not just the maturity of each component but also their integration into a cohesive design. While the components have been individually tested and are designed for compatibility with commercially available CubeSat systems, the integration of these components into a unified system has not yet been realized. Given that the components have not been integrated and tested as a single, cohesive system, the overall system can be currently considered at TRL 3.

Therefore, although the concept of the design is deemed feasible based on individual component tests and their intended compatibility with standard CubeSat platforms, there is still significant work to be done before the system can be considered mission-ready. This work includes not only the further development and testing of the capture mechanism, but also comprehensive testing of the integrated system under conditions that closely resemble those it will encounter in space.

The use of CubeSats as a low-cost alternative to larger, more complex spacecraft presents a financially viable solution for deploying de-orbiting missions in LEO. For instance, considering a commercially available CubeSat system like the AstroDigital Corvus 6 bus, with a mass of approximately 12 kilograms including payload, companies such as RocketLab can launch these CubeSats into LEO at around $5 million per launch, or about $22,000 per kilogram [39]. With the cost per satellite valued at around $1.3 million, a mission involving three such spacecraft targeting a specific piece of debris would incur a cost of roughly $4.7 million. This is a relatively modest amount, especially when compared to the potential billions of dollars in damages that unmitigated space debris could cause.

SpaceX further enhances the cost-effectiveness of such missions, offering an even more competitive price of around $2,645 per kilogram [39]. Therefore, between the purchase of launch vehicle at around $70 million and other moderately priced larger spacecraft, or a swarm of ten or more de-orbit spacecraft, this mission could be funded for around $100 million – a striking contrast to the expenses associated with large, sophisticated spacecraft.

While launch costs are a significant portion of the total expense, they are not the only costs involved in such missions. Additional expenses include the development and testing of the spacecraft, mission control operations, and post-mission analysis. However, the overarching conclusion remains that utilizing CubeSats for debris removal missions could be executed at a fraction of the cost required for larger, more intricate spacecraft.

B. FUTURE WORK

Areas of future work for enhancing and refining the design presented in this study centers primarily on the development of the capture mechanism. Key areas for improvement include the utilization of more durable materials in its construction and conducting more rigorous testing under operational conditions. These steps are crucial for ensuring the mechanism's reliability and effectiveness in the challenging environment of space. Additionally, integrating this refined capture mechanism into a commercially available CubeSat platform is an essential milestone. This integration process will test the compatibility of the mechanism with standard CubeSat systems and help in identifying any adjustments needed for optimal performance.

Another important consideration for improvement is the ability to reset the mechanism in the event of an unsuccessful capture. This ability to reset is crucial for several reasons. Firstly, incorporating a robust trigger mechanism is essential. This mechanism should be designed to withstand the harsh conditions of space and be resilient enough to maintain functionality after a missed capture attempt, ensuring that the system remains operational for subsequent attempts. Secondly, integrating a strong reeling system is equally important. This system would be responsible for retracting the projectile back to the spacecraft after a missed shot. A reliable reeling system would facilitate multiple capture attempts, enhancing the overall efficiency of the mission. The significance of these improvements becomes particularly evident when considering the high costs associated with launching payloads into orbit. A design that allows for multiple capture attempts – as opposed to a single-use design – greatly improves the return on investment. By enabling the spacecraft to reset and retry capturing debris, the mission's success rate can be significantly increased, making the most of the resources spent on launching and operating the spacecraft.

Another important area for future research involves a more detailed analysis of the EDT using advanced tether simulation software. Such software can provide deeper insights into the dynamics of the tether's interaction with the Earth's magnetic field and other environmental factors in space. This analysis would enhance the understanding of the EDT's performance and could lead to further improvements in its design.

An intriguing aspect that warrants exploration is the correlation between fluctuations in solar activity and variations in the orbital decay rate, as observed in NPSAT-1. Solar activity can significantly impact the space environment, affecting factors like atmospheric density, which in turn influences the rate of orbital decay. Studying this relationship could yield valuable information for predicting and managing the behavior of satellites and debris in orbit.

Furthermore, the study did not address the maneuvers required for a spacecraft to rendezvous with debris objects. Investigating the navigational and control aspects needed for such rendezvous operations is a complex but fascinating area of research. It involves challenges such as trajectory planning, guidance algorithms, and fuel optimization, all of which are critical for successful debris capture missions.

Considering the uncontrolled nature of de-orbiting large, heavy orbital debris using these methods, there’s a notable risk that parts of this debris could survive reentry and pose safety hazards. This situation necessitates a detailed study on safety measures for such de-orbiting methods. Such a study could assess the probability of debris surviving reentry, predict potential impact zones, and explore risk minimization strategies.

Finally, an exciting avenue for future work is the design of a mission that utilizes the payloads developed in this study. This mission would involve not only the deployment of the improved capture mechanism and EDT but also the integration of these systems into a comprehensive mission plan. This plan would encompass aspects such as target selection, mission timelines, and the coordination of multiple spacecraft, providing a practical application of the study’s findings and contributing to efforts in space debris mitigation.

THIS PAGE INTENTIONALLY LEFT BLANK

LIST OF REFERENCES

[1] G. S. Aglietti *et al.*, "The active space debris removal mission Removedebris. Part 2: in orbit operations," *Acta Astronaut.*, vol. 168, pp. 310–322, Mar. 2020, doi: 10.1016/j.actaastro.2019.09.001.

[2] M. Shan, J. Guo, and E. Gill, "Review and comparison of active space debris capturing and removal methods," *Prog. Aerosp. Sci.*, vol. 80, pp. 18–32, Jan. 2016, doi: 10.1016/j.paerosci.2015.11.001.

[3] M. L. Verbeeck, "Drag enhancement device prototype for mid-size spacecraft," M.S. Thesis, Dept. of Mech. and Aerosp. Eng., NPS, Monterey, CA, USA, 2019 [Online]. Available: https://calhoun.nps.edu/handle/10945/62699

[4] A. C. Long and D. A. Spencer, "A scalable drag sail for the deorbit of small satellites," *JoSS*, vol. 7, no. 3, pp. 773–778, Jan. 2019.

[5] S. J. Nichols, "De-orbiting drag sail," M.S. Thesis, Dept. of Mech. and Aerosp. Eng., NPS, Monterey, CA, USA, 2020 [Online]. Available: https://calhoun.nps.edu/handle/10945/65410

[6] D. McKnight *et al.*, "Identifying the 50 statistically-most-concerning derelict objects in LEO," *Acta Astronaut.*, vol. 181, pp. 282–291, Apr. 2021, doi: 10.1016/j.actaastro.2021.01.021.

[7] K. Wormnes *et al.*, "European Space Agency (ESA) technologies for space debris remediation," in *6th European Conference on Space Debris*, 2013 [Online]. Available: https://conference.sdo.esoc.esa.int/proceedings/sdc6/paper/116

[8] J.-C. Liou and N. L. Johnson, "Risks in space from orbiting debris," *Science*, vol. 311, no. 5759, pp. 340–341, Jan. 2006, doi: 10.1126/science.1121337.

[9] B. Virgili and H. Krag, "Analyzing the criteria for a stable environment," in *Advances in the Astronautical Sciences*, 2011 [Online]. Available: https://www.researchgate.net/publication/266556917

[10] D. J. Kessler, N. L. Johnson, J.-C. Liou, and M. Matney, "The Kessler syndrome: Implications to future space operations," in *33rd Annual AAS Guidance and Control Conference*, 2010 [Online]. Available: https://citeseerx.ist.psu.edu/document/10-016

[11] 18th and 19th Space Defense Squadron, *Spaceflight Safety Handbook for Satellite Operators*, 1.7. Combined Force Space Component Command, 2023 [Online]. Available: https://www.space-track.org/documents/SFS_Handbook_For_Operators_V1.7.pdf

[12] National Aeronautics and Space Administration, “Handbook for limiting orbital debris.” 2018 [Online]. Available: https://standards.nasa.gov/sites/default/files/standards/NASA/Baseline/1/nasa-hdbk-871914_baseline_with_change_1.pdf

[13] European Space Agency, “ESA space debris office.” Accessed: Jul. 23, 2023 [Online]. Available: https://www.esa.int/Enabling_Support/Operations/Ground_Systems_Engineering/ESA_Space_Debris_Office

[14] LeoLabs, “Leotrack,” LeoLabs. Accessed: Jul. 23, 2023 [Online]. Available: https://leolabs.space/leotrack/

[15] United Nations Committee on the Peaceful Uses of Outer Space, “Report of the committee on the peaceful uses of outer space,” United Nations, New York, N.Y, General Assembly Official Records A/77/20, Jun. 2022 [Online]. Available: https://documents-dds-ny.un.org/doc/UNDOC/GEN/221/025/6E

[16] M. Metz, “Inter-Agency Space Debris Coordination Committee (IADC).” Accessed: Jul. 23, 2023 [Online]. Available: https://www.iadc-home.org/what_iadc

[17] D. A. Vallado and D. Finkleman, “A critical assessment of satellite drag and atmospheric density modeling,” *Acta Astronaut.*, vol. 95, pp. 141–165, Feb. 2014, doi: 10.1016/j.actaastro.2013.10.005.

[18] D. L. Oltrogge and K. Leveque, “An evaluation of cubesat orbital decay,” in *25th Annual AIAA/USU Conference on Smalll Satellites*, 2011 [Online]. Available: https://digitalcommons.usu.edu/cgi/article=1144

[19] J. M. Picone, A. E. Hedin, D. P. Drob, and A. C. Aikin, “NRLMSISE-00 empirical model of the atmosphere: Statistical comparisons and scientific issues,” *J. Geophys. Res. Space Phys.*, vol. 107, no. A12, p. SIA 15–1-SIA 15–16, 2002, doi: 10.1029/2002JA009430.

[20] S. Bruinsma and C. Boniface, “The operational and research DTM-2020 thermosphere models,” *J. Space Weather Space Clim.*, vol. 11, p. 47, 2021, doi: 10.1051/swsc/2021032.

[21] A. C. Keith and J. Baker PhD, “A non-technical overview and discussion of rendezvous and proximity operations (RPO),” U.S. AFRL, Kirtland AFB, NM, USA, TOR-2013-01086, 2013.

[22] D. Ivanov, M. Kushniruk, and M. Ovchinnikov, “Study of satellite formation flying control using differential lift and drag,” *Acta Astronaut.*, vol. 152, pp. 88–100, Nov. 2018, doi: 10.1016/j.actaastro.2018.07.047.

[23] Biesbroek, Robin, Soares, Tiago, Huesing, Jakob, and Innocenti, Luisa, "The e.deorbit CDF study: A design study for the safe removal of large space debris," in *6th European Conference on Space Debris*, 2013. Accessed: Oct. 09, 2023 [Online]. Available: https://conference.sdo.esoc.esa.int/proceedings/sdc6/paper/122

[24] Reed, Jaime and Barraclough, Simon, "Development of harpoon system for capturing space debris," in *6th European Conference on Space Debris*, 2013. Accessed: Apr. 28, 2023 [Online]. Available: https://conference.sdo.esoc.esa.int/proceedings/sdc6/paper/27/SDC6-paper27.pdf

[25] R. Dudziak, S. Tuttle, and S. Barraclough, "Harpoon technology development for the active removal of space debris," *Adv. Space Res.*, vol. 56, no. 3, pp. 509–527, Aug. 2015, doi: 10.1016/j.asr.2015.04.012.

[26] A. Majid, M. N. Owais, and M. N. Qureshi, "Aerodynamic drag computation of Lower Earth Orbit (LEO) satellites," *J. Space Technol.*, vol. 8, no. 1, pp. 82–89, Jul. 2018.

[27] R. Hoyt, "Terminator tape: A cost-effective de-orbit module for end-of-life disposal of LEO satellites," in *AIAA SPACE 2009 Conference & Exposition*, 2009. doi: 10.2514/6.2009-6733.

[28] H. M. James and E. Guth, "Theory of the elastic properties of rubber," *J. Chem. Phys.*, vol. 11, no. 10, pp. 455–481, Oct. 1943, doi: 10.1063/1.1723785.

[29] G. W. Prolss, *Physics of the Earth's space environment: an introduction*. Berlin ; New York: Springer, 2004.

[30] D. Halliday, R. Resnick, and J. Walker, *Fundamentals of physics*, 10th ed. Danvers, MA, USA: John Wiley and Sons, 2014.

[31] R. L. Forward, R. P. Hoyt, and C. W. Uphoff, "Terminator tether: A spacecraft deorbit device," *J. Spacecr. Rockets*, vol. 37, no. 2, pp. 187–196, Mar. 2000.

[32] G. Borderes-Motta *et al.*, "Cross-verification and benchmarking analysis of electrodynamic tether simulators," *Acta Astronaut.*, pp. 381–388, Jul. 2023.

[33] R. Forward, R. Hoyt, and C. Uphoff, "Application of the terminator tether electrodynamic drag technology to the deorbit of constellation spacecraft," in *34th AIAA/ASME/SAE/ASEE Joint Propulsion Conference and Exhibit*, 1998 [Online]. Available: https://arc.aiaa.org/doi/10.2514/6.1998-3491

[34] J. Stroup, "NPSAT1: Assessment of risk for human casualty from atmospheric reentry," M.S. Thesis, Dept. of Mech. and Aerosp. Eng., NPS, Monterey, CA, USA, 2016 [Online]. Available: http://hdl.handle.net/10945/48481

[35] H. C. Stankey and R. P. Hoyt, "In-flight performance of the terminator tape end-of-life deorbit module."

[36] A. G. Demoss, "Optimized trajectories for satellite formation flying using differential drag maneuvers," M.S. Thesis, Dept. of Mech. and Aerosp. Eng., NPS, Monterey, CA, USA, 2023 [Online]. Available: https://hdl.handle.net/10945/72344

[37] S. Caldwell, "State-of-the-art of small spacecraft technology," NASA [Online]. Available: https://www.nasa.gov/smallsat-institute/sst-soa/introduction/

[38] C. Manning, "Technology readiness levels – NASA," NASA. Accessed: Nov. 30, 2023 [Online]. Available: https://www.nasa.gov/directorates/somd/space-communications-navigation-program/technology-readiness-levels/

[39] D. Chow, "How falling launch costs are fueling the thriving space industry," *NBC News*, Apr. 08, 2022. Accessed: Dec. 05, 2023 [Online]. Available: https://www.nbcnews.com/science/space/space-launch-costs-growing-business-industry-rcna23488

INITIAL DISTRIBUTION LIST

1. Defense Technical Information Center
   Ft. Belvoir, Virginia

2. Dudley Knox Library
   Naval Postgraduate School
   Monterey, California